Semiannual Phase Report No. 2

LEAD TELLURIDE BONDING AND SEGMENTATION STUDY

Covering period

February 1 - July 31, 1968

Contract No. NAS 5-9149

Prepared by

Tyco Laboratories, Inc.

Bear Hill

Waltham, Massachusetts 02154

for

National Aeronautics and Space Administration

Goddard Space Flight Center

Greenbelt, Maryland 20771

Tyco Laboratories, Inc.
Bear Hill
Waltham, Massachusetts 02154

Lead Telluride Bonding and Segmentation Study

Semiannual Phase Report No. 2

Covering period
February 1 - July 31, 1968

Contract No. NAS 5-9149

by

H. Bates
F. Wald
M. Weinstein

for

National Aeronautics and Space Administration
Goddard Space Flight Center
Greenbelt, Maryland 20771

SUMMARY

This report presents constitutional results on the Co-Si-Ge system and the PbTe-MnTe system. In substantial detail, life testing of elements and couples is discussed, and data for couples tested over 2900 hours under gradient conditions are shown.

CONTENTS

CONTENTS (Cont.)

LIST OF ILLUSTRATIONS

LIST OF ILLUSTRATIONS (cont.)

LIST OF ILLUSTRATIONS (cont.)

LIST OF TABLES

I. INTRODUCTION

The widespread use of thermoelectric power generation has been anticipated for some years as the solution to a number of specialized power-supply problems. However, the application of thermoelectrics has been hindered by a number of major materials problems. These problems can be divided into those associated with (1) the physical characteristics, (2) the chemical behavior, and (3) the low conversion efficiency of thermoelectric materials.

The predominantly covalent nature of most thermoelectric alloys results in materials which are generally weak and brittle. In addition, PbTe alloys have a high thermal expansion coefficient which leads to susceptibility to thermal shock and thermal stress cracking. The mismatch in expansion coefficient between PbTe and metals also causes a fundamental physical incompatability which must be dealt with in contacting these materials at the hot side. The vapor pressure of PbTe alloys precludes operation in vacuum or requires encapsulation. Porosity in sintered PbTe not only contributes to its mechanical instability, but may also pose a substantial long-term hazard to the integrity of metallurgical bonds by migration of the pores in the temperature gradient. The high temperature mechanical properties of PbTe alloys are very poorly defined, and there is almost a complete lack of understanding as to what role they may have in generator design.

The reactive nature of one or more elements in all thermoelectric materials places severe limitations on the materials for use as hot side contacts. Reaction between the metal contact and the thermoelectric material can produce electrically active or mechanically destructive phases at the interface. Interactions between the dopants and contacts, which can drastically affect the electrical properties, are also possible. In fact, the consequences of reaction between the thermoelectric material and any of the several materials which constitute its environment are such that extreme care must be exercised in the choice of all such materials. However, without a basic knowledge of the interactions of the thermoelectric

material with metals, potential brazes, insulations, and so forth, selection of these materials can only be by a trial and error process.

The low efficiency of thermoelectric generating materials has been the main impediment to their wider application as power sources. The search for new materials has been largely abandoned. However, the need for higher efficiencies still exists. The most feasible means for achieving higher efficiencies appears to be the combination of existing materials over extended temperature ranges. The best known thermoelectric power generation materials, PbTe and Si-Ge, have optimum temperature ranges which complement each other for operation over a temperature interval of 800 - 1000°C to 200 - 50°C. Devices utilizing these materials over such a temperature interval should exhibit higher conversion efficiency than either material alone.

This program comprises a study of (1) the bonding of PbTe thermoelements to nonmagnetic electrodes, (2) the behavior of the elements and contacts at operational temperatures, (3) the compatibility of PbTe and SnTe with metals and the interactions of Si-Ge thermoelectric materials with potential hot contact materials and brazes, and (4) the physical and chemical characteristics of the PbTe thermoelements. Other aspects of the program include a study of the segmenting of Si-Ge thermoelements with PbTe for higher efficiency, life testing of PbTe thermoelements and couples, design and construction of a prototype test device for Si-Ge-PbTe thermocouples, and the design of modules incorporating W-bonded PbTe and segmented SiGe-PbTe.

The general aim of the program is to define the most appropriate system and process for the preparation of low-resistance, high strength bonds of nonmagnetic electrodes to PbTe alloys and to study the factors and processes involved in the degradation of thermoelements and contacts during extended service.

II. CONSTITUTIONAL STUDIES

A. Metal-Silicon-Germanium Systems

1. Introduction

In the first semiannual phase report on the present contract a background study of the literature on metal-silicon-germanium systems was presented. Also results of preliminary microprobe studies on cast alloys containing 2% metal were discussed, and experimental difficulties likely to be encountered in such systems were pointed out. In the following a more detailed description of parts of the Co-Ge-Si system is presented in the form of nonequilibrium binary sections and an equilibrium ternary isothermal plane for high Ge-Si concentrations at 760°C.

2. Alloy Preparation and Experimental Procedures

All alloys were prepared from electrolyte cobalt and semiconductor purity silicon and germanium.

Because of the difficulties of dissolving silicon in the alloys, most of them were premelted in an argon arc furnace. The charges were usually about 20 grams in size and were also checked at times for weight losses after melting. Such losses were usually found to be negligibly small.

Thermal analysis investigations were carried out in the apparatus described in various reports and papers written under this contract. Metallographic and X-ray investigations were carried out by standard techniques except that lattice parameters and error limits on them were computed electronically as described in the first semiannual phase report for the case of the SnTe-Metal alloys.

3. Results

a. $CoSi_2$-2 Ge (Nonequilibrium, Nonpseudobinary) Section. Four alloys containing 25, 50, 75 and 90 mol % Ge_2 were

prepared. A nonequilibrium thermal section was not established here, since the alloys cross several different phase fields. Representative photomicrographs of as-cast alloys are shown in Figs. 1 and 2.

b. CoSi-2 Ge (Nonequilibrium, Nonpseudobinary) Section. Five alloys containing 25, 33 1/3, 50, 75 and 90 mol % Ge_2 were prepared. Alloys are situated in substantially the same phase field.

The nonequilibrium thermal section is shown in Fig. 3 and a representative photomicrograph of an as-cast alloy in Fig. 4.

c. CoSi-CoGe-Section. Since CoSi-CoGe alloys play a very important role in the determination of the ternary system, it is therefore necessary to describe the constitution of these alloys in somewhat more detail. Figure 5 shows the nonequilibrium section as determined by thermal analysis on as-cast speciments and also gives the positions of the alloys on the section.

Figures 6 and 7 show two representative microphotographs of the nonequilibrium structures, the alloy with 50 mol % CoGe, and the alloy with 70 mol % CoGe. Three phases are apparent in both of them. It is also clear from the thermal results that the section is to be divided into two parts; apparently the peritectic formation of CoGe plays a role in the two alloys with the highest CoGe concentrations.

The three alloys not showing thermal effects below 900°C were annealed for 864 hours at that temperature. The other two have been annealed for 2586 hours at 760°C.

Investigation of the three alloys annealed at 900°C (10, 30 and 50 mol % CoGe) showed them to be single phased (Fig. 8). X-ray measurements revealed CoSi with shifted cubic lattice constants increasing with increasing Ge contents (Fig. 9). The two alloys annealed at 760°C appeared two phase (Fig. 10).

Fig. 1 $(CoSi_2)_{.1}(2Ge)_{.9}$ as cast, polarized light. 700 X

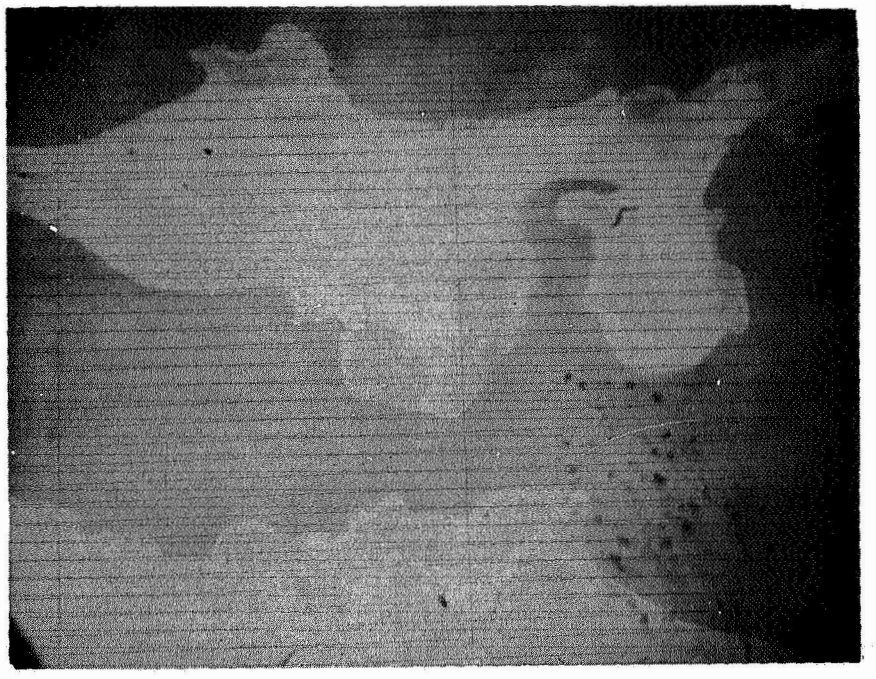

Fig. 2 $(CoSi_2)_{.75}(2Ge)_{.25}$ as cast, polarized light. 700 X

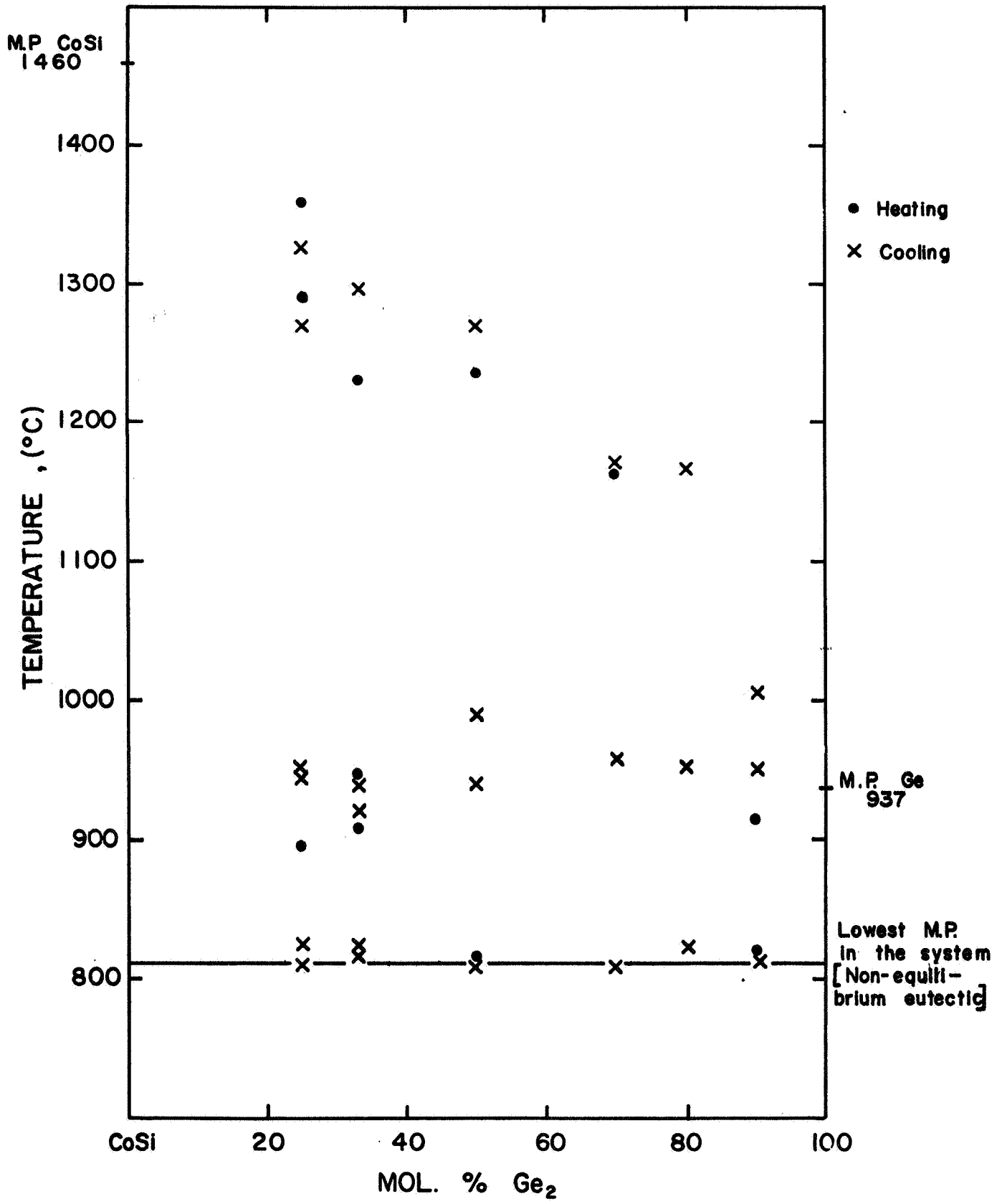

Fig. 3 Nonequilibrium section of the CoSi-2Ge alloys.
(● = thermal arrests on heating)
(x = thermal arrests on cooling)

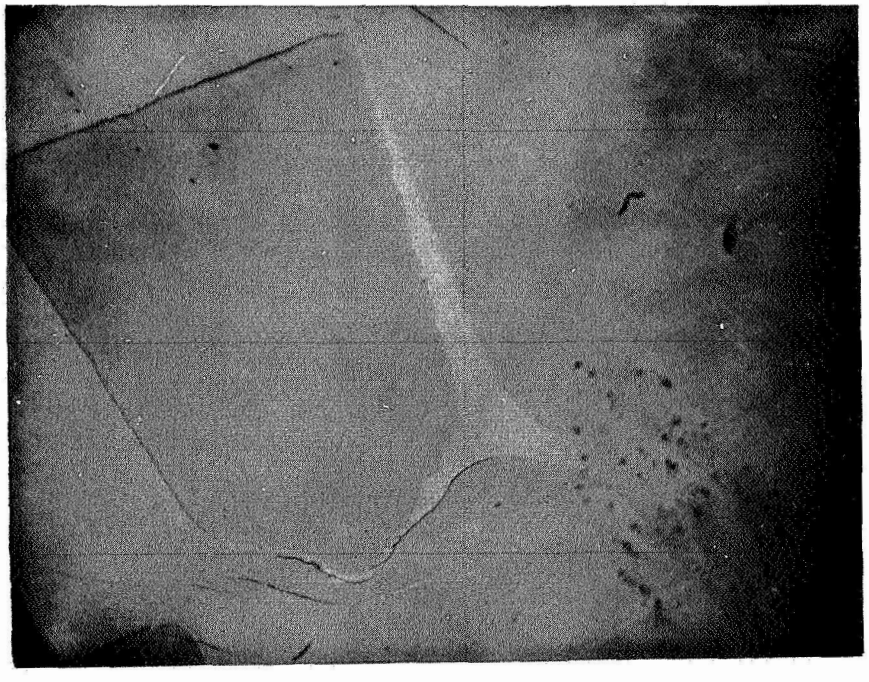

Fig. 4 $(CoSi)_{.5}(2Ge)_{.5}$ as cast, polarized light. 700 X

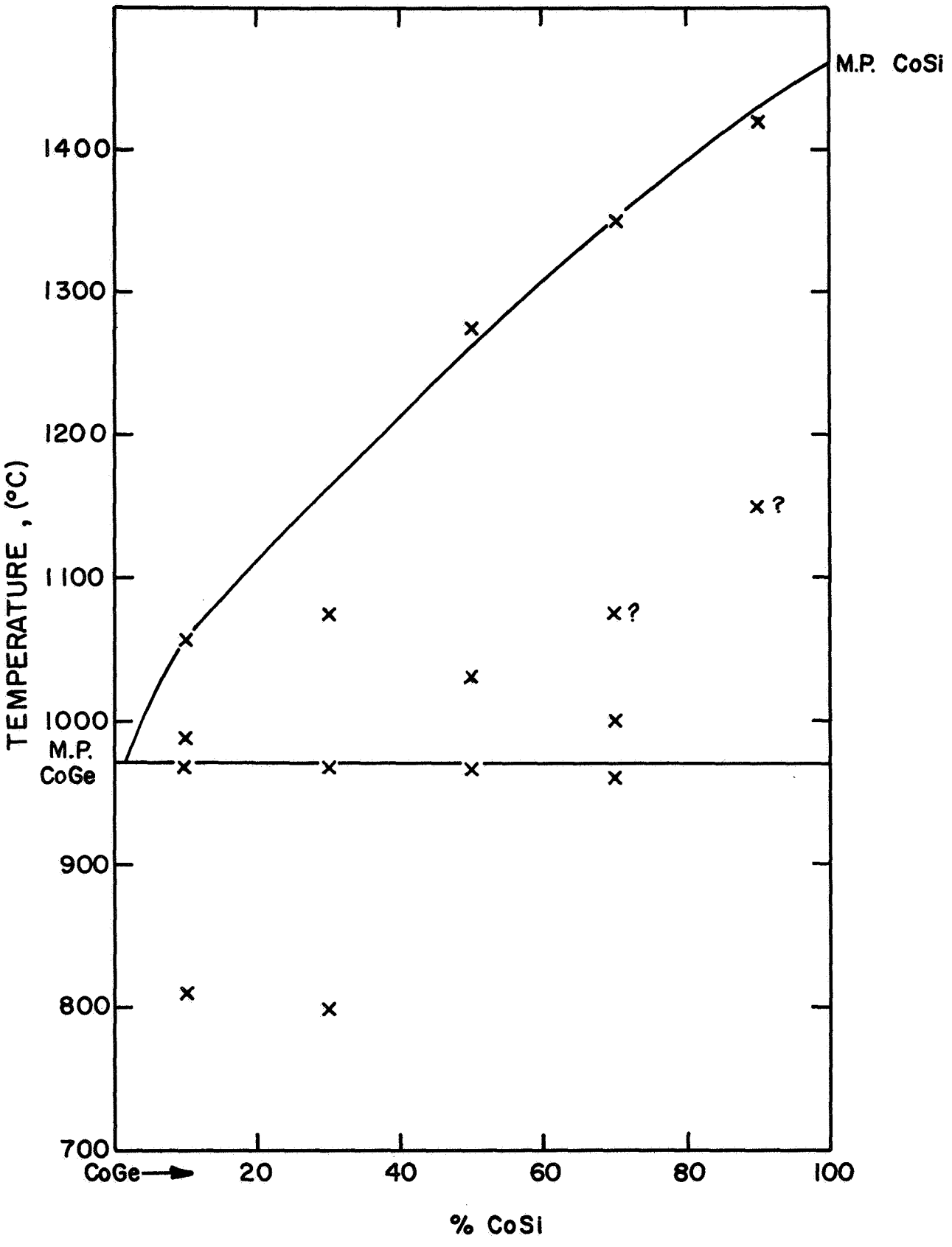

Fig. 5 Nonequilibrium thermal section of the CoGe-CoSi alloys.

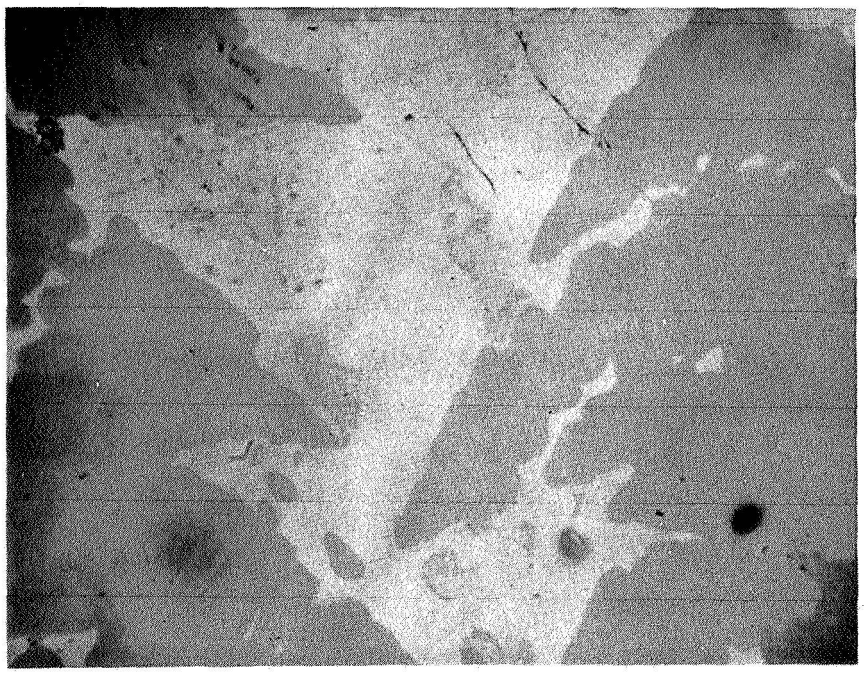

Fig. 6 $(CoSi)_{.5}(CoGe)_{.5}$ as cast, polarized light. Note appearance of three phases. 700 X

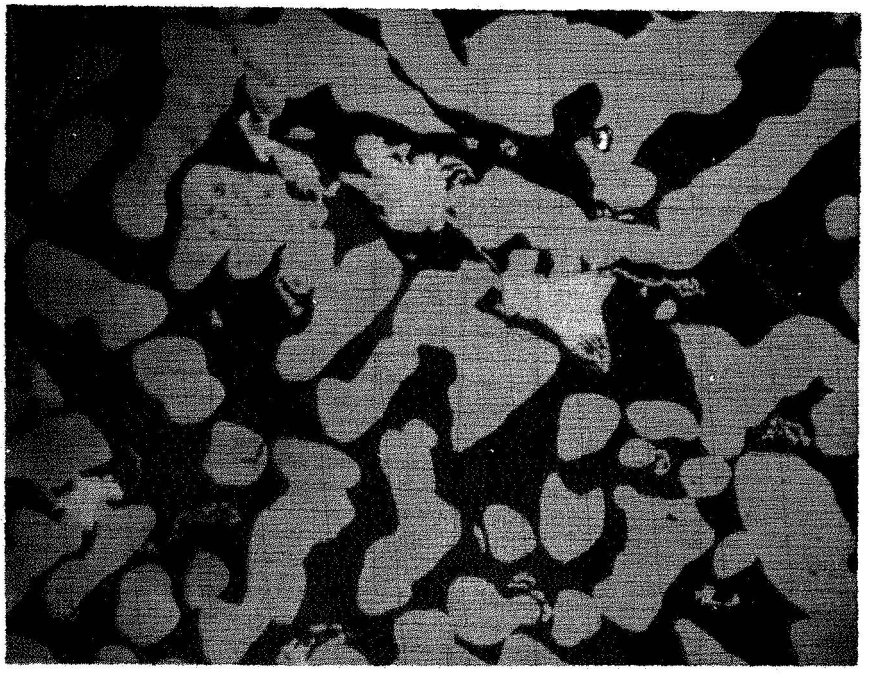

Fig. 7 $(CoSi)_{.3}(CoGe)_{.7}$ as cast, polarized light. Note appearance of three phases. 700 X

Fig. 8 $(CoSi)_{.5}(CoGe)_{.5}$ 864 hours, 900°C, polarized light. Note single phase appearance. 700 X

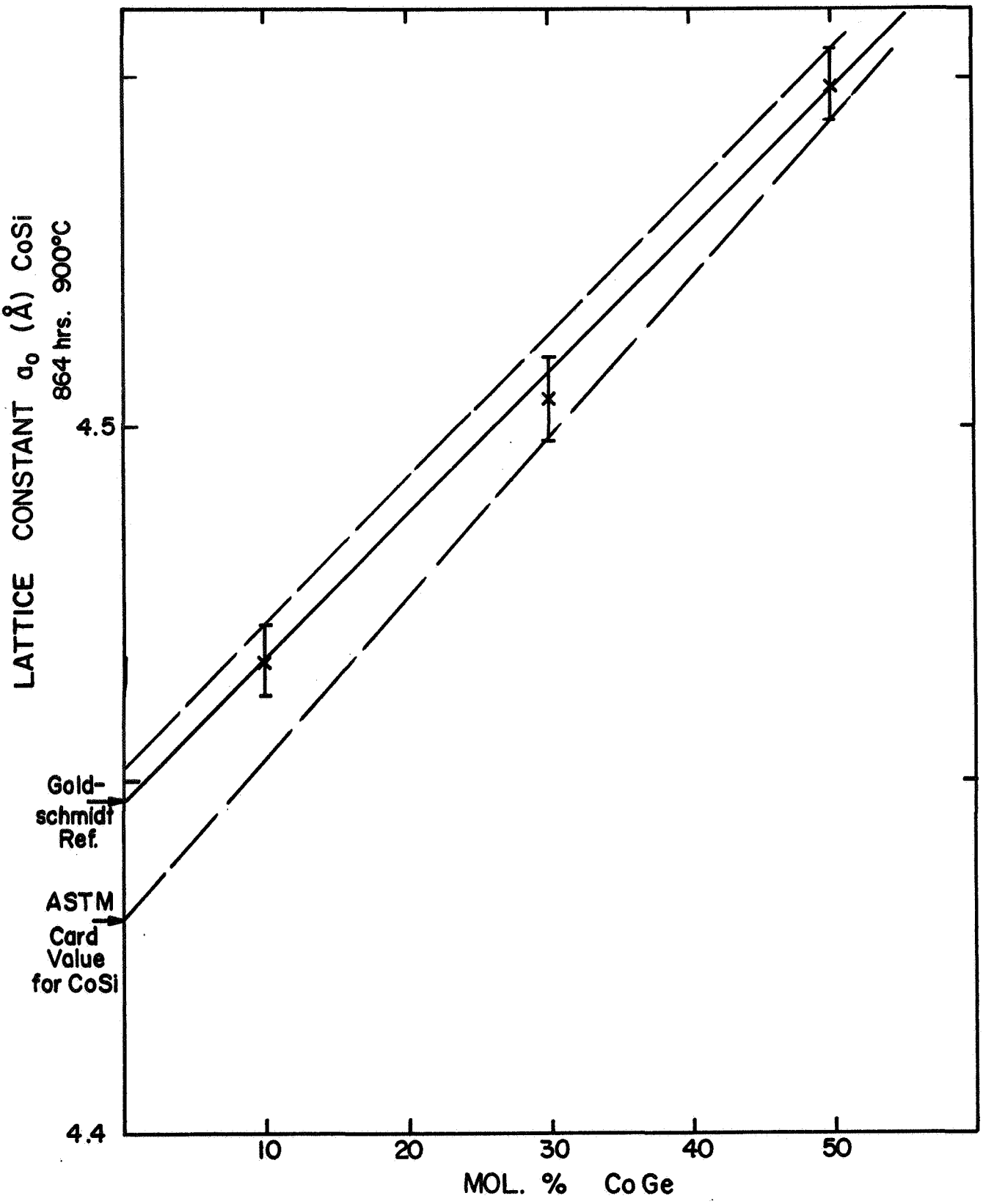

Fig. 9 Cubic lattice constants of CoSi-CoGe solid solutions. ✱ = error limits. (Goldschmidt, ref. 2, tabulates the lattice parameters of all cobalt-silicides.)

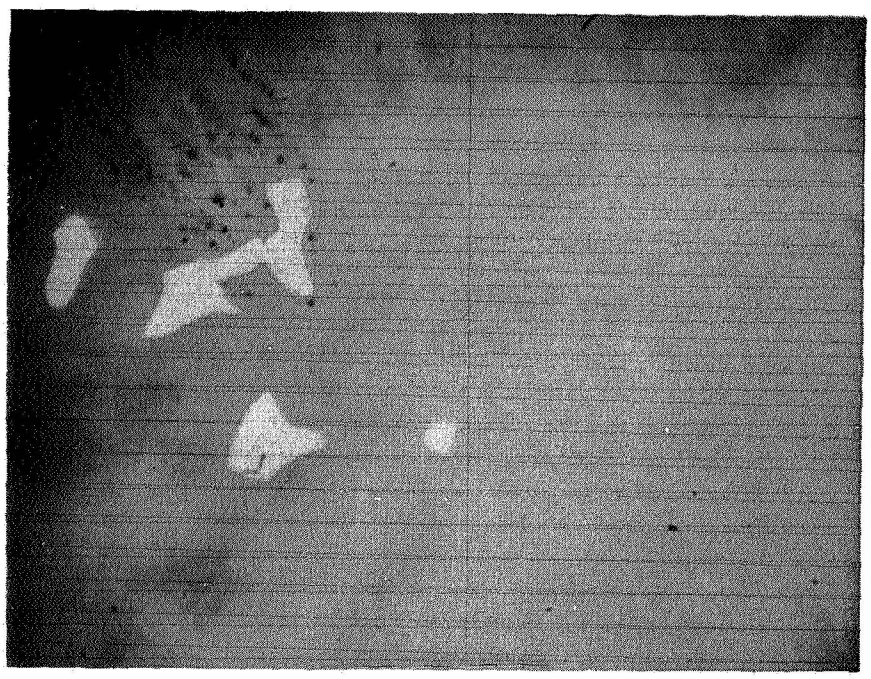

Fig. 10 $(CoSi)_{.3}(CoGe)_{.7}$ 2586 hours, 750°C, polarized light. Note appearance of only two phases. 700 X

From the combined results it appears that the section might be pseudobinary, with a large solid solubility of CoGe in CoSi (up to at least 50 mol %), followed perhaps by a eutectic or peritectic reaction at higher CoGe concentrations. However, this latter point needs confirmation.

d. The Ternary Range CoSi-CoGe-Ge-Si at 760°C. All alloys of the CoSi-Ge_2 section and the $CoSi_2$-Ge_2 section have been annealed for more than 1000 hours at 760°C.

From an evaluation of these alloys by X-ray analysis and optical microscopy (considering also the results on the CoSi-CoGe section), a reasonably clear picture of the constitutional principles governing the system at high Ge-Si concentrations emerged.

To support the final conclusions, in Table I all X-ray results are presented and in Fig.11 the lattice constants of the Ge-Si solid solutions are presented as extrapolated from the results of Hassion, et al.[1]. Also Figs. 12-14 present some of the microstructures encountered in these alloys.

From the combined results the phase diagram shown in Fig. 15 emerges. As can be seen however, various gaps which require detailed quantitative verification, are readily apparent.

e. Conclusions. Although a good idea of the principles of constitution in the Co-Ge-Si system has emerged, it can by no means be considered complete. Several steps are planned which should aid in establishing a complete phase diagram of the system. A number of additional alloys have to be made and investigated. These are shown as circles in Fig. 16, which shows the alloys already investigated as X's. Also, thermal analysis runs on preannealed alloys have to be made to establish the temperatures of equilibrium phase reactions. In addition, longer annealing of the alloys in the far Ge corner is necessary, since they are probably not yet in equilibrium.

TABLE I

X-Ray Results on Co-Si-Ge Alloys

CoSi-CoGe 864 hrs. 900°C

Composition	Microscopy	a_o CoSi (Å)	Remarks
$(CoSi)_{.9}(CoGe)_{.1}$	Single Phase	4.467 ± 0.005	Single Phase X-ray
$(CoSi)_{.7}(CoGe)_{.3}$	Single Phase	4.504 ± 0.006	Single Phase X-ray
$(CoSi)_{.5}(CoGe)_{.5}$	Single Phase	4.549 ± 0.005	Single Phase X-ray

$CoSi_2$-2Ge (1300 hrs. 700°C) 1550 hrs. 760°C

Composition	Microscopy	a_o CoSi (Å)	a_o $CoSi_2$ (Å)	a_o GeSi (Å)	Remarks
$(CoSi_2)_{.75}(2Ge)_{.25}$	3-Phase	4.449 ± 0.007	5.371 ± 0.005	5.59 ± 0.01	--
$(CoSi_2)_{.50}(2Ge)_{.50}$	3-Phase	4.445 ± 0.007	5.374 ± 0.005	5.594 ± 0.008	--
$(CoSi_2)_{.25}(2Ge)_{.75}$	2 (3?) Phase	4.432 ± 0.005	--	5.65 ± 0.02	X-ray $CoGe_2$ present ?
$(CoSi_2)_{.10}(2Ge)_{.90}$	3-Phase	4.45 ± 0.01	--	5.656 ± 0.003	X-ray $CoGe_2$ present ?

CoSi-2Ge 1090 hrs. 760°C

Composition	Microscopy	a_o CoSi (Å)	a_o GeSi (Å)	Remarks
$(CoSi)_{.75}(2Ge)_{.25}$	2-Phase	4.451 ± 0.004	5.654 ± 0.004	--
$(CoSi)_{.66}(2Ge)_{.33}$	2-Phase	4.455 ± 0.004	5.652 ± 0.004	--
$(CoSi)_{.50}(2Ge)_{.50}$	2-Phase	4.454 ± 0.004	5.649 ± 0.005	--
$(CoSi)_{.25}(2Ge)_{.75}$	2-Phase	4.471 ± 0.006	5.654 ± 0.001	X-ray $CoGe_2$ present ?
$(CoSi)_{.10}(2Ge)_{.90}$	3-Phase ?	4.48 ± 0.01	5.654 ± 0.002	X-ray $CoGe_2$ present

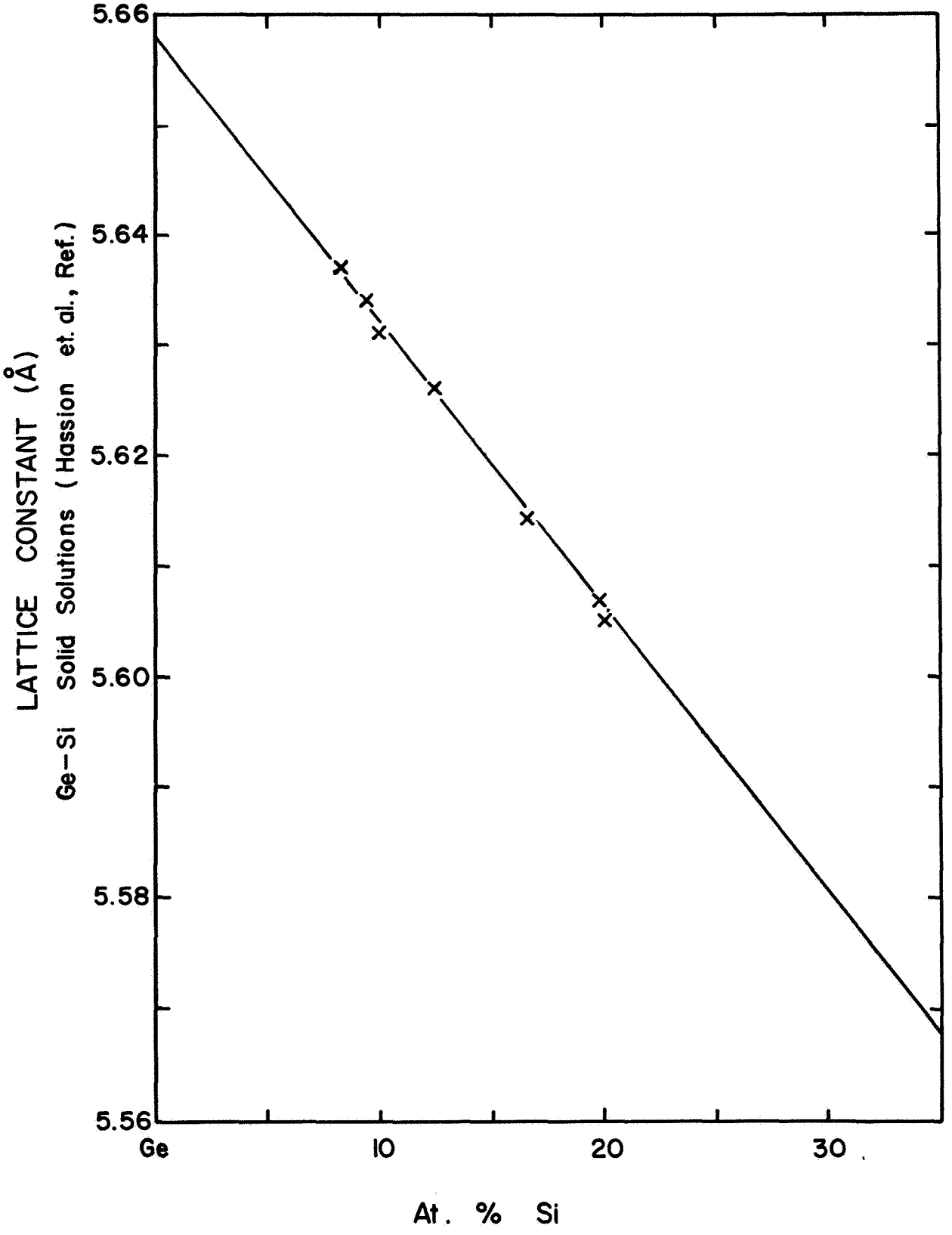

Fig. 11 Lattice constants of germanium-silicon solid solutions (after Hassion, et al., ref. 1).

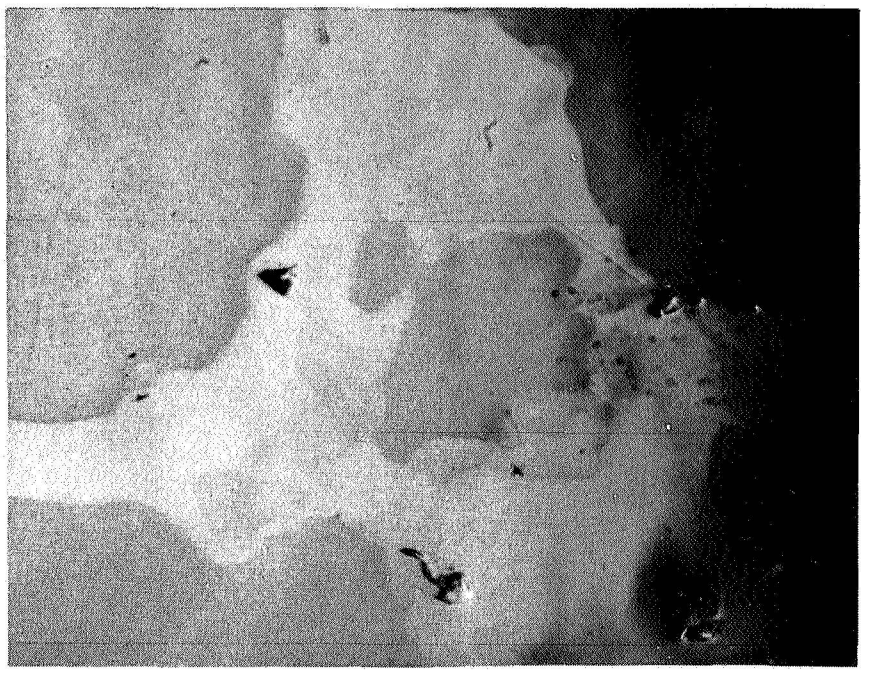

Fig. 12 $(CoSi_2)_{.75}(2Ge)_{.25}$ 1550 hours, 760°C, polarized light. Three phases are clearly visible. 700 X

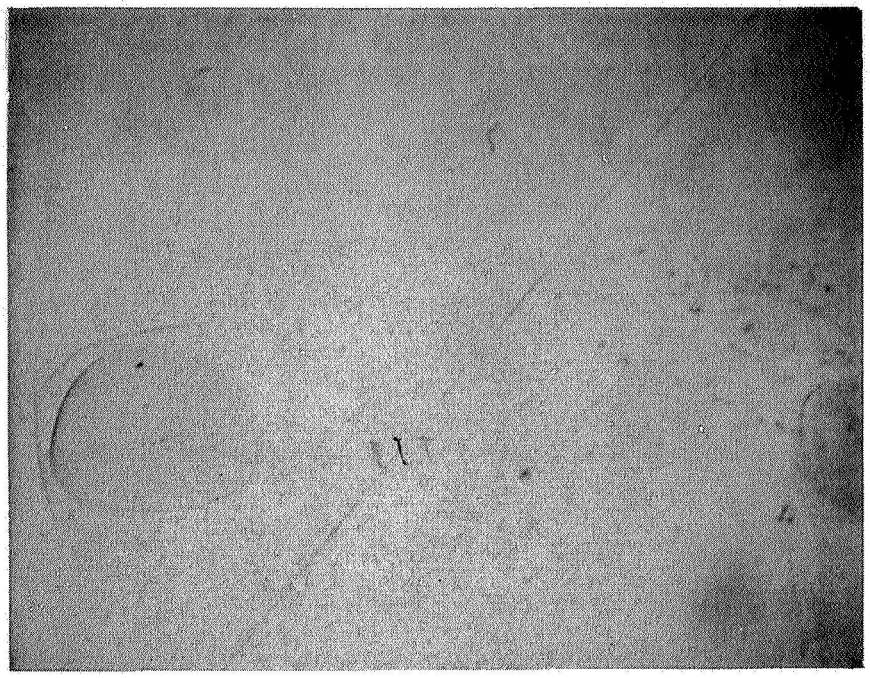

Fig. 13 $(CoSi)_{.25}(2\,Ge)_{.75}$ 1090 hours, 760°C, polarized light. Note the two-phase appearance. 700 X

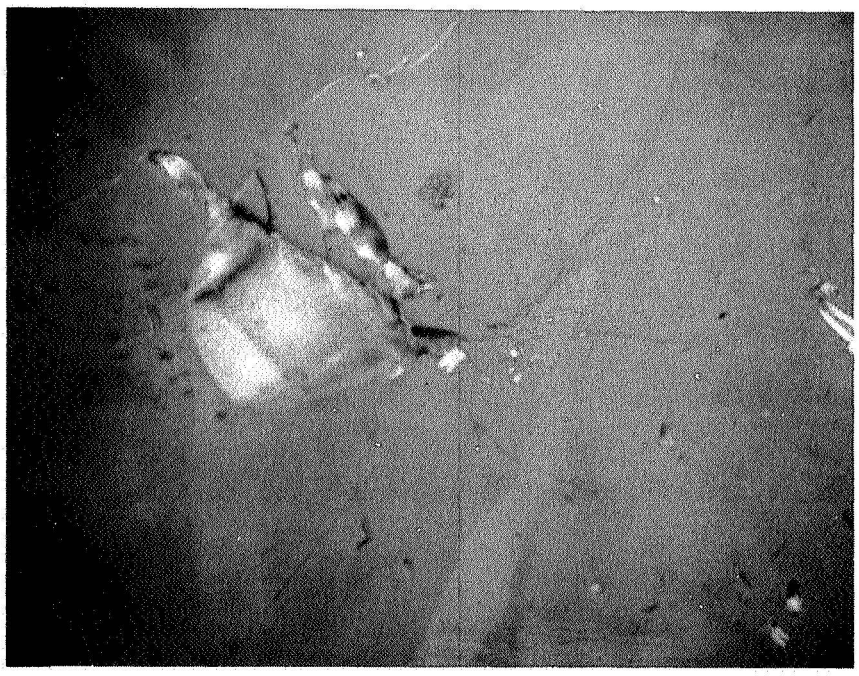

Fig. 14 $(CoSi_2)_{.10}(2Ge)_{.90}$ 1550 hours, 760°C, polarized light. Three phases are visible, but equilibrium has probably still not been attained. 700 X

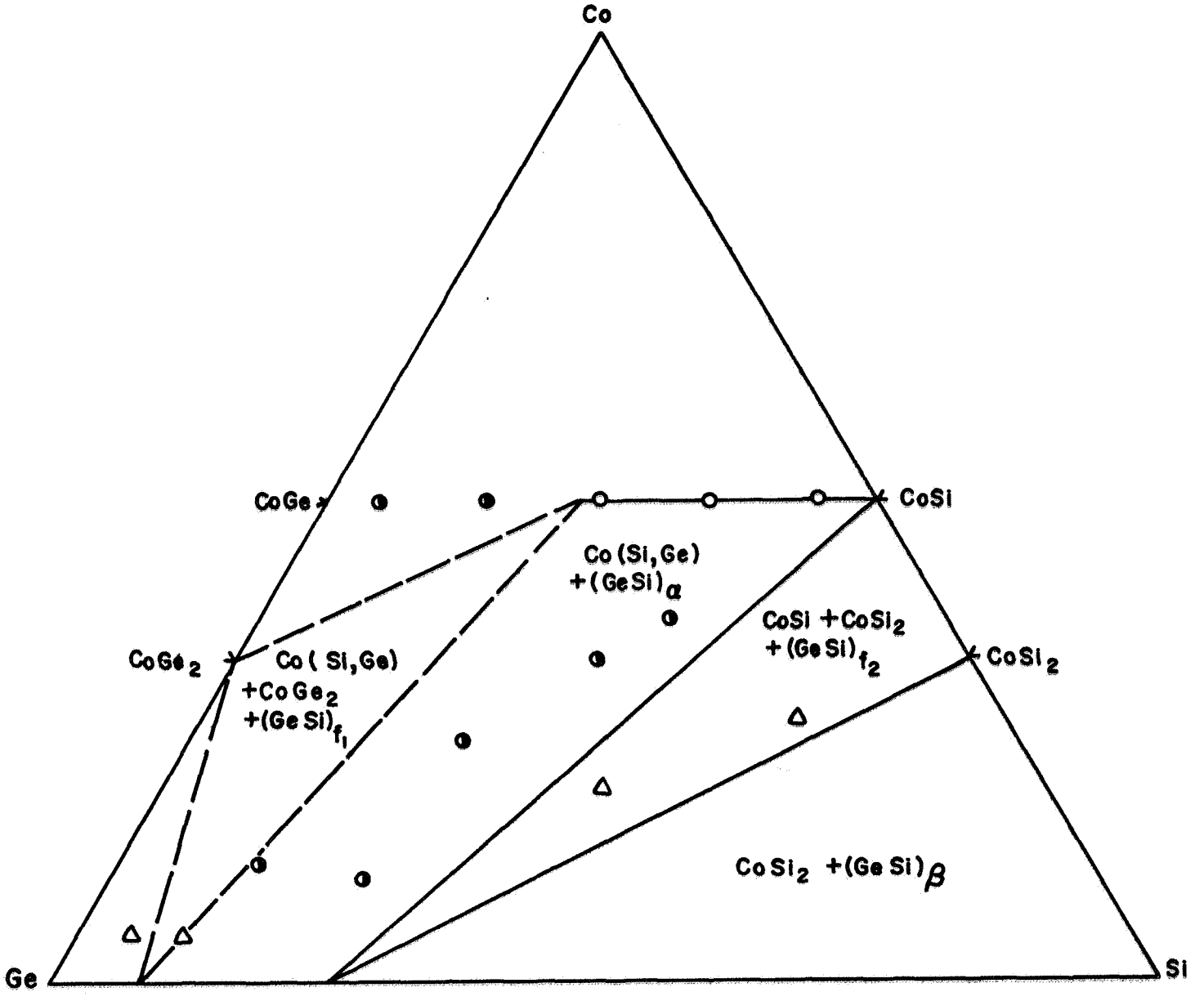

Fig. 15 Preliminary phase diagram of Co-Ge-Si alloys with high silicon and germanium concentrations (isothermal plane at 760°C; o = points at 900°C).

Phase Designations:

o = single phase, ◑ = two phase, Δ = three phase
$\alpha + \beta$ = Ge-Si solid solutions of variable concentrations
$f_1 + f_2$ = Ge-Si solid solutions of fixed concentrations.

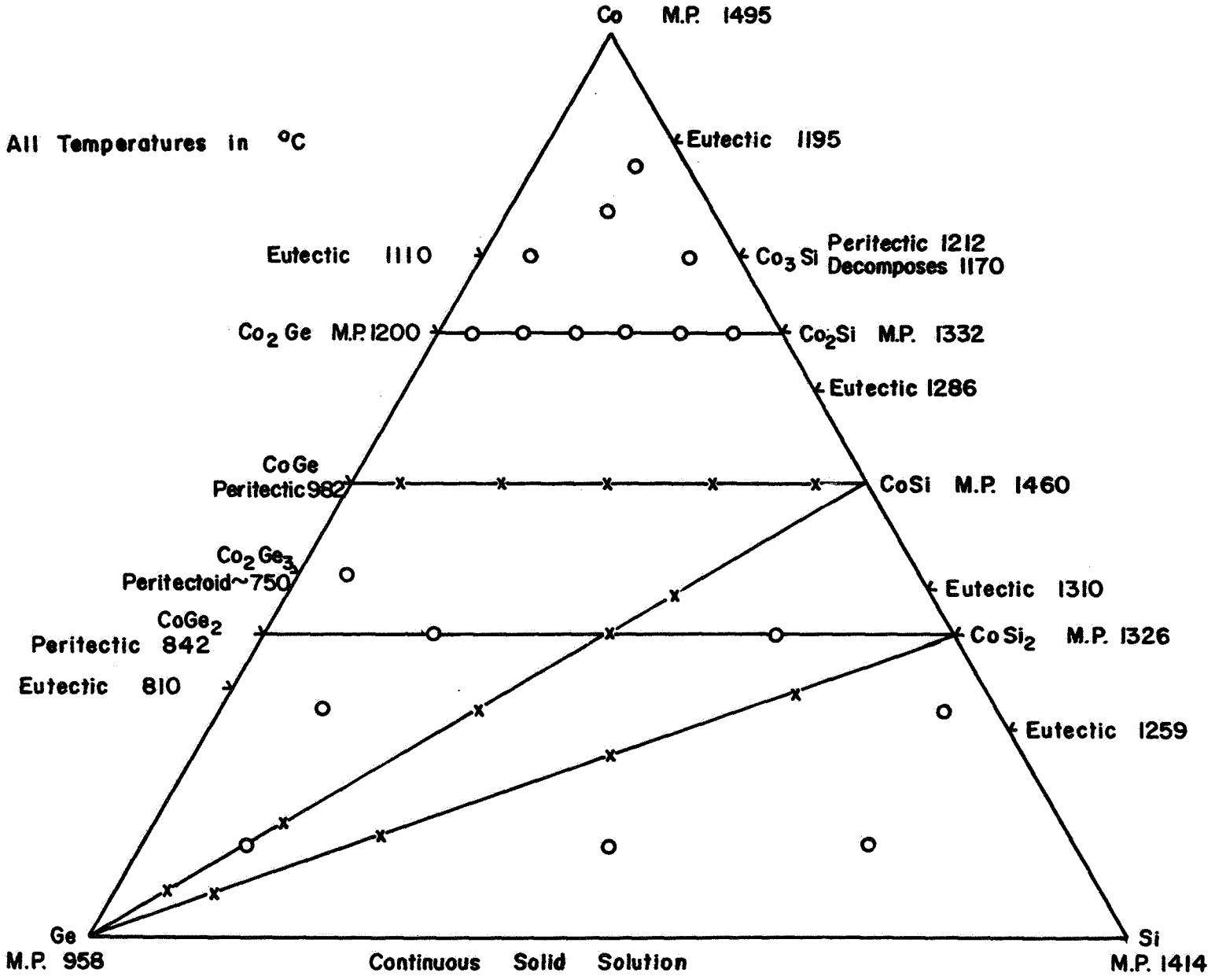

Fig. 16 Alloys in the cobalt silicon-germanium system.

Important points so far established are as follows:

(1) CoSi at 900°C dissolves at least up to 50 mol % CoGe as a cubic solid solution.

(2) $CoSi_2$ does not dissolve any appreciable amounts of $CoGe_2$.

(3) CoSi-CoGe solid solutions of high Si contents are in equilibrium with Ge-Si solid solutions of high Ge contents.

(4) CoSi and $CoSi_2$ form a ternary equilibrium with a Ge-Si solid solution of $25 \pm 5\%$ Si content.

B. Diffusion

Of rather substantial interest in contacting thermoelectric materials are various questions related to diffusion.

This is notably true for thermoelectric materials containing free tellurium excesses. From simple considerations of chemical equilibrium it becomes clear that sooner or later reaction of the metal contacts with the tellurium excess will lead to the establishment of telluride layers in the contact zone.

Further growth of these layers and therefore the rate of depletion of Te from the thermoelectric material will then obviously depend on the speed of transfer of the reactants through the initial layer. Thus a passivating layer is desirable.

Since it is known that, in general, the self diffusion of the lower melting constituents is the fastest[3], the diffusion of Te through the telluride layer is to be considered. Not too much is known about the diffusion of Te in metal tellurides; (a good summary can be found in Hagel' s paper[3]). One important factor becomes rather clear: To a large extent slow diffusion is coupled with a minimization of vacancy content[3]. This is true because it seems reasonable to assume that Te does not diffuse over interstitials. Then, in fundamental terms[4] the self diffusion constant is given by.

$$D = g \nu p_s \cdot p_e$$

Here, g is a geometric constant, ν is a vibrational frequency, p_s is the probability that the species of interest in the diffusion process is next to a suitable site, and p_e is the probability that the diffusing species has enough energy to surmount the energy barrier between its present site and an adjacent site.

This latter term may be expressed in terms of the melting temperature of the diffusing species and its crystallographic environment, including its valency:[3]

$$D = a \exp (- b T m/T)$$

Thus we have:

$$D = g \nu p_s (\exp (-b Tm/T))$$

Now, g, ν, b and the melting point may, if we are looking at the same diffusing species in a similar environment, all be considered as constants. We then obtain:

$$D = k_1 p_s (\exp k_2)$$

Here it can then be seen that the diffusion of Te becomes dependent on p_s, which can be equated with the vacancy concentration of the telluride formed, i. e. its phase lattitude. That this is indeed true may be seen from ref. (3).

By consultation of metal-tellurium phase equilibrium data, it can be decided which metals form tellurides with the smallest phase lattitudes (ideally stoichiometric line phases). These should have the lowest diffusion coefficients.

If, for instance, iron and tungsten are compared, it can be seen that all iron tellurides contain substantial phase lattitudes[5, 6], wheras tungsten telluride constitutes substantially a line phase[7]. Thus, Te-diffusion through WTe_2 should be very slow.

Another, thermomechanical, requirement for a passivating layer also arises. Within the temperature of interest it should be mechanically compatible, i. e. not crack on cycling, etc. There are no data on the thermal expansion compatibility of either iron tellurides or tungsten telluride. However, the fact that two of the known iron tellurides decompose on cooling below 488°C[5] introduces an additional stress on cooling which might lead to cracking of the junctions in which these iron tellurides are present.

C. The Manganese Telluride-Lead Telluride Section

1. Introduction

In another chapter of this report, the influence of life tests under gradient conditions on 3 P-type thermoelectric material is described. It is well-known that this material is constituted of PbTe, SnTe, MnTe, free Te and perhaps Mn, the latter obviously being introduced as a getter and consequently to be found in the consolidated thermoelectric material as MnO inclusions. So far as is known to the authors, no phase equilibrium information on either the two binary systems containing MnTe or the ternary system is to be found in the literature, with the exception of the paper of Chomentowski, et al.[8], which gives the solubility limit of MnTe in PbTe only (lower than 3 mol % at 500°C).

It would appear in view of the metallurgical changes in the 3P material, to be interesting to have some detailed information on the PbTe-SnTe-MnTe system, including the effects of varied excess Te. Knowledge of the metallurgical and electrical behavior of that system would probably materially aid in the understanding of the changes in the electrical parameters of 3P material under operating conditions and perhaps allow the composition of that material to be changed to one which is more suitable.

Preliminary to the investigation of the ternary system it is necessary to investigate the constituent binary equilibria. The PbTe-SnTe system is, of all the binaries involved, the only one

reasonably well-known[9, 10, 11, 12]. As mentioned before a small part of the PbTe-MnTe system has been superficially studied[8]. No studies on the SnTe-MnTe system have apparently been reported.

Certain results on MnTe itself and on the MnTe-GeTe and MnTe-MnSe system are relevant here. They are reported in papers by Johansen[13], Johnston and Sestrich[14] and Panson and Johnston[15]. Points of interest in these papers are the description of the hexagonal to cubic transformation of MnTe at 1039°C and studies on equilibria between the sodium-chloride structure type (or very nearly so) compounds GeTe or MnSe on the one side and MnTe with its NiAs-NaCl type transformation.

2. Experimental

The experiments were carried out in the usual manner with ~ 20 g charges prepared from electrolytic manganese and semiconductor pure lead and tellurium.

The quartz capsules used had to be coated with graphite to prevent wetting and subsequent cracking on cooling. Thermal analysis and X-ray investigations were carried out in the usual manner, as were metallographic observations. Microscopic hot stage investigations under ~ 1.5 atm argon pressure were used but were not successful because of excessive evaporation at all temperatures above ~ 550°C.

3. Results

From the initial thermal analysis runs the phase diagram presented in Fig. 17 was constructed.

The general outline, consisting of the formation of a continuous solid solution series with a minimum melting point and a monotectoid and subsequent eutectoid reaction, so far seems to be the only reasonable construction to be made from the thermal analysis points. This construction apparently is supported by the microstructures of cast alloys which definitely show four distinct areas as exemplified in Figs. 18-21, namely:

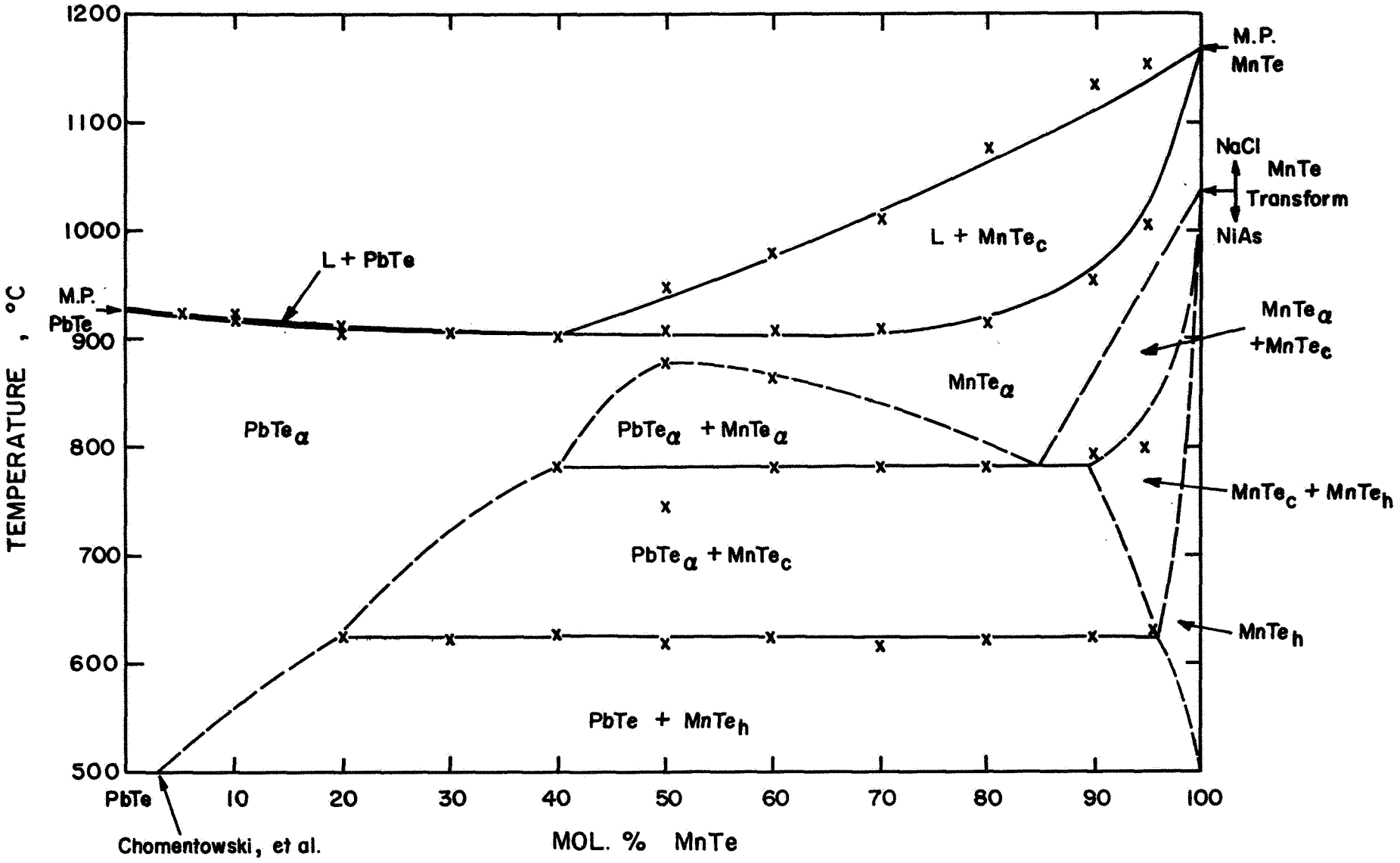
1200
1100
1000
900
800
700
600
500
TEMPERATURE , °C
M.P.
PbTe
M.P.
MnTe
NaCl
MnTe
Transform
NiAs
L + PbTe
L + MnTe$_c$
MnTe$_\alpha$
+MnTe$_c$
MnTe$_\alpha$
PbTe$_\alpha$
PbTe$_\alpha$ + MnTe$_\alpha$
MnTe$_c$ + MnTe$_h$
PbTe$_\alpha$ + MnTe$_c$
MnTe$_h$
PbTe + MnTe$_h$
PbTe
10
20
30
40
50
60
70
80
90
100
Chomentowski, et al.
MOL. % MnTe

Fig. 17

Fig. 17 Preliminary phase diagram of the pseudobinary system lead telluride-manganese telluride, based on thermal analysis results and microscopic observations on as-cast specimens.

Phase Designations:

$PbTe_{\alpha}$ = Sodium chloride structure type solid solution of PbTe-MnTe with high PbTe content and variable composition.

$MnTe_{\alpha}$ = Sodium chloride structure type solid solution of MnTe-PbTe with high MnTe content and variable composition.

PbTe = Terminal solid solution of sodium chloride structure type PbTe.

$MnTe_{c}$ = Terminal Solid solution of sodium chloride structure type (high temperature form)MnTe.

$MnTe_{h}$ = Terminal solid solution of hexagonal NiAs type (low temperature form) MnTe.

(All thermal arrests were averaged from at least two heating and cooling points.)

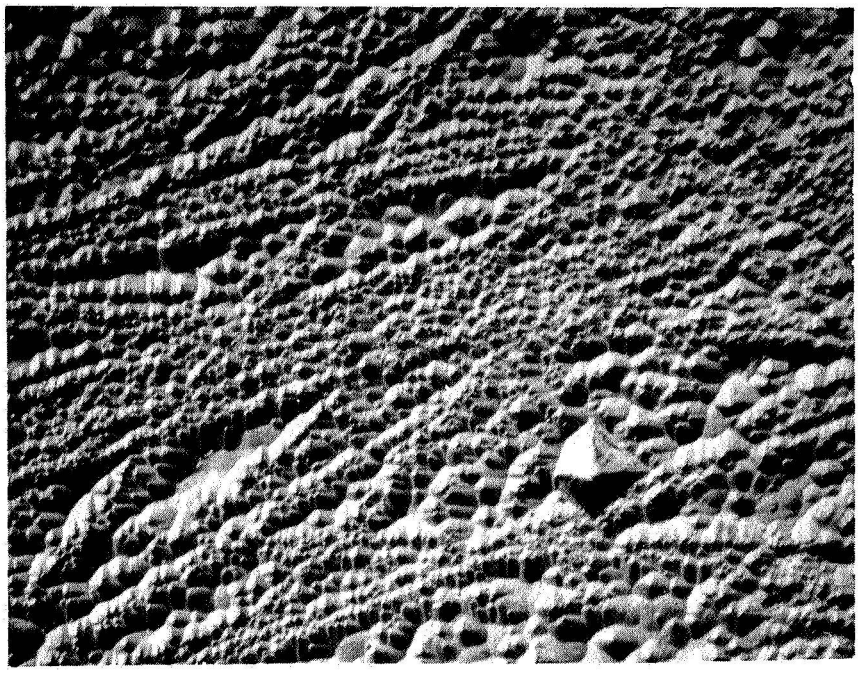

Fig. 18 95 mol % PbTe - 5 mol % MnTe (0.84 weight % Mn), as cast, Murakami etch. 1000 X

The charge consists merely of 3 or 4 large single phased grains with no indication of second phase precipitates. However, the extreme etch pit density within the grains indicates rather imperfect crystalline behavior, a fact that may be related to pre-precipitation phenomena such as extreme lattice disorder. The etch pits, when evaluated by light figure techniques, reveal 4-fold symmetry.

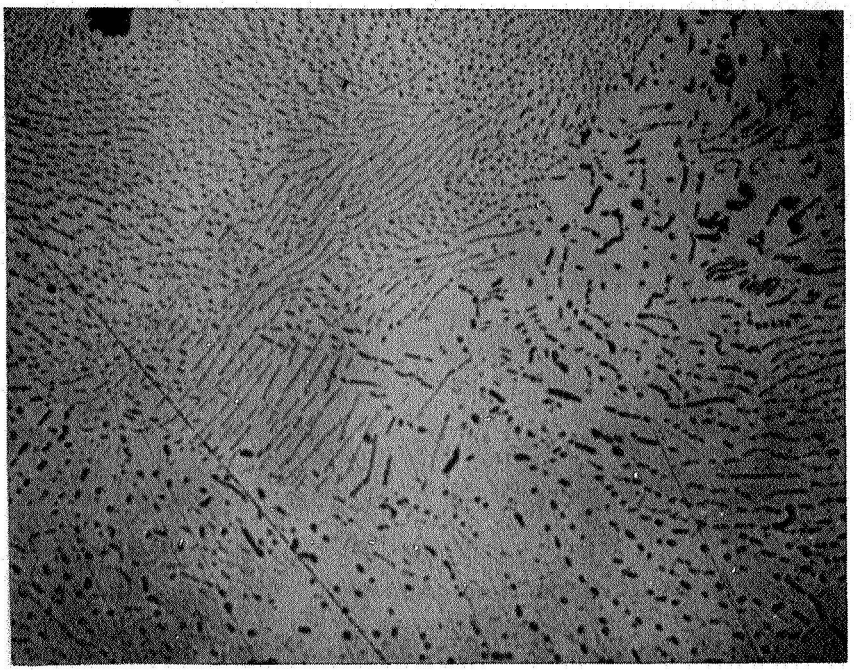

Fig. 19 80 mol % PbTe - 20 mol % MnTe (3.6 weight % Mn), as cast, polarized light. An apparently eutectoidal structure is clearly visible here. 1000 X

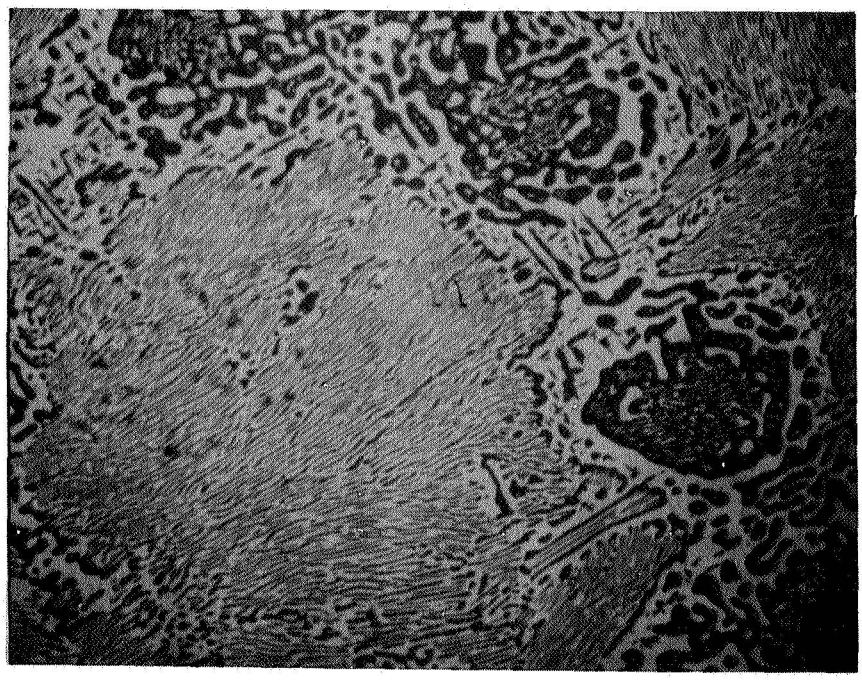

Fig. 20 50 mol % PbTe - 50 mol % MnTe (10.6 weight % Mn), as cast, polarized light. An apparently eutectoidal structure interspersed with droplike inclusions indicates monotectoid behavior. 1000 X

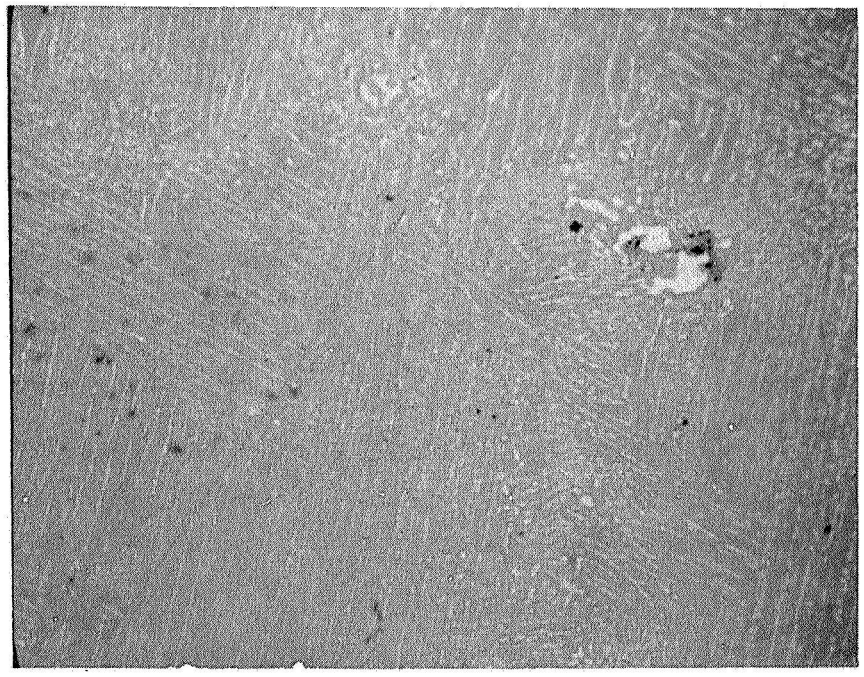

Fig. 21 10 mol % PbTe - 90 mol % MnTe (25 weight % Mn), as cast, polarized light. Primary matrix and lamellar precipitates indicate hypermonotectoid region. 1000 X

(1) A single phase solid solution at 5 mol % MnTe.
(2) A clearly eutectoidal structure between 10 and 40 mol % MnTe.
(3) A eutectoidal structure with round inclusions at 50 to 80 mol % MnTe.
(4) A matrix with aligned solid state precipitates at 90 and 95 mol % MnTe.

4. Discussion

The complexity of the system becomes quite obvious from the microstructures; thus the phase diagram presented must be considered as preliminary. Trials to quench the transformations have completely failed, and hot stage investigations are impossible because of the high vapor pressures and evaporation rates in the system.

Complete confirmation can be achieved only by high temperature X-ray investigations in a heated Debye-Scherrer camera in which a sample can be contained in a quartz capillary to inhibit evaporation.

Presently under investigation are the solubility limits on both sides of the phase field which can be obtained by annealing and quenching methods and subsequent X-ray lattice parameter measurements. Furthermore, since the solid state transformations often showed only small and indefinite effects in direct thermal analysis, differential methods are to be used in repeat runs on all alloys.

5. Conclusions

The lead telluride-manganese telluride system has been found to behave in a rather complex manner. Substantial further information is needed to establish a reasonable phase diagram. It may be suggested, however, that the ternary PbTe-SnTe-MnTe diagram is probably equally complex and thus the complicated behavior of 3P materials in temperature gradients over long times is not altogether surprising.

III. ISOTHERMAL LIFE TESTING

Measurements have been made on a number of 3P W-bonded elements after testing at 525°C for periods of 1100, 1700, and 7300 hours. This represents about 192,000 test hours on some 56 3P-W junctions and about 141,000 test hours on 51 3P elements (bonded and unbonded). A small number of 2P and 3N elements have also been tested.

A. 7300-Hour Test of W-bonded 3P Elements

A group of ten bonded elements and two unbonded controls were measured after accumulating a total of 7300 hours at 525°C. These elements had been measured after 1000 hours originally and then held for 6300 additional hours. The element and contact resistance for this group of samples are tabulated in Table II.

Five contacts failed completely, while four were unmeasurable because of cracking of four of the elements. From the average values of Table III it can be seen that the contacts which were intact at the end of 7300 hours have increased in resistance approximately 2.4 times. It can also be seen that these contacts represented the "better" contacts both initially and at 1000 hours, the resistance of the ten being about 10% below the over-all average at 1000 hours and 5% below the over-all average initially. This lends some substantiation to our feeling that the lower the initial resistance of a contact, the better its lifetime performance should be.

One other point to be drawn from the information on contact resistance is the following: If the ten contacts intact at 7300 hours are considered, a rate of increase in contact resistance can be calculated. For the first 1000 hours this rate is 15 $\mu\Omega$/1000 hours. Over the following 6300 hours the rate is 14 $\mu\Omega$/1000 hours. Whether or not this represents the rate of some real, basic process of change in the contacts remains to be seen. The over-all rate of contact resistance change, that is for all the elements intact at 1000 hours in the group tested to 7300

TABLE II

Element and Contact Resistances of W-bonded 3P Elements Tested at 525°C for 7300 Hours

Element	C.R.$_T$ μΩ	C.R.$_B$ μΩ	Element mΩ	C.R.$_T$ μΩ	C.R.$_B$ μΩ	Element mΩ	C.R.$_T$ μΩ	C.R.$_B$ μΩ	Element mΩ
6L1P30	85	60	1.755	125	35	2.02	-	580	2.22
6L3P30	95	60	1.795	145	100	1.94	-	x	x
6L4P30	110	70	1.720	90	75	2.04	-	120	1.97
6M1P30	95	60	1.795	100	70	2.08	x	140	x
6M2P30	80	55	1.815	90	55	2.11	200	130	2.17
6M3P30	85	50	1.665	95	80	2.03	--	200	1.95
6M6P30	90	75	1.735	130	70	1.95	230	100	2.12
611P15	95	75	1.830	200	70	x	x	130	x
612P15	75	60	1.870	x	85	x	x	-	x
615P30	70	100	1.830	140	100	2.04	320	190	2.09
P25-1	--	--	1.690			1.96			2.20
P25-2	--	--	2.050			1.90			2.20

x Indicates cracked or broken element, but intact bond.

- Failed or initially missing contact.

TABLE III

Summary of Average Contact and Element Resistances for W-bonded 3P Elements Tested 7300 hours at 525°C

	Initial	1000 hrs	7300 hrs
Average contact resistance, $\mu\Omega$	77	---	---
(nineteen contacts)	77	98	---
(ten contacts)	73	88	176
Average bonded element resistance, m Ω	1.785	---	---
(eight elements)	1.765	2.04	---
(six elements)	1.76	2.03	2.09
Average control element resistance, m Ω	1.87	1.93	2.20
Average bonded element Seebeck voltage vs. Cu, mv	70	70.5	68.5

hours, was 22 $\mu\Omega$/ 1000 hours. Similar rates calculated for groups of elements tested to 2000 and 3000 hours are 38 $\mu\Omega$/ 1000 hours and 29 $\mu\Omega$/ 1000 hours, respectively. This gives some indication that the behavior of long-lived contacts is not simply a low initial resistance, but also an apparently lower degradation rate.

The room temperature element resistance averages are also listed in Table III. The increase in resistance after isothermal testing has been demonstrated a number of times previously. What these figures do show is that the major amount of increase apparently occurs within the first 1000 hours. This was not entirely clear from the previous tests at 1000, 2000, and 3000 hours. What is not shown by these figures is perhaps more important than the increase in element resistance (which does not hold true in gradient testing in any case) and that is the number of elements which failed by cracking. It has been pointed out before that this is a strong indication for the desirability of compressive loading on any PbTe structure.

The Seebeck voltage shows a small decrease over the 6300-hour period. This decrease of 2 mv is negligible when compared with the decreases in Seebeck voltage, as a result of metallurgical changes, found in gradient tested elements.

B. 1700-Hour Test of W-bonded 3P Elements

A group of twelve bonded and six unbonded control elements were tested initially for 1700 hours. The main purpose of this test was to attempt to show clearly any possible differences in behavior of elements from two different purchase lots of material. Element and contact resistances are listed in Table IV, and average properties for the two groups are listed in Table V.

It is apparent from these data that the performance of these elements is not particularly good. The contacts have increased 2.5 times in a short period; the rate of increase is

TABLE IV

Element and Contact Resistances of W-bonded 3P Elements
Tested at 525°C for 1700 Hours

	0 Hours			1700 Hours		
Element	$C.R._T$	$C.R._B$	Element	$C.R._T$	$C.R._B$	Element
	$\mu\ \Omega$	$\mu\ \Omega$	m Ω	$\mu\ \Omega$	$\mu\ \Omega$	m Ω
7I9 P37	100	80	1.81	270	120	2.21
7I7 P37	125	70	1.87	225	65	2.06
7I13 P37	50	100	1.87	1100	700	1.90
7I8 P37	100	50	1.85	210	x	x
7I14 P37	105	135	1.69	145	130	1.93
7I15 P37	180	60	1.73	-	600	2.40
7I5 P37	175	200	1.78	170	x	1.78
7I2 P37	-	80	1.87	-	175	2.16
7H8 P33A	105	70	1.85	-	-	1.65
7H15 P33A	-	60	1.96	-	360	2.16
7H18 P33A	150	150	2.05	260	x	x
7H17 P33A	-	80	2.13	-	130	1.87
31 P37			2.19			2.30
34 P37			1.95			2.40
35 P37			1.96			2.35
3 P33A			2.01			2.60
4 P33A			1.85			2.45
5 P33A			1.92			2.20

x Indicates cracked or broken element, but intact bond.

- Failed or initially missing contact.

TABLE V

Average Properties of 1700 Hour Tested Elements-Comparison

	0 hours	1700 hours
P37		
Average contact resistance (11 bonds) $\mu\Omega$	102	255
Average bonded element resistance, m Ω	1.80	2.06
Average bonded element Seebeck voltage, mv	69	66
Average control element resistance, m Ω	2.00	2.35
Average control element Seebeck voltage, mv	70	72
P33A		
Average contact resistance (3 bonds) $\mu\Omega$	97	250
Average bonded element resistance, m Ω	1.98	1.89
Average bonded element Seebeck voltage, mv	70	65
Average control element resistance, m Ω	1.93	2.41
Average control element Seebeck voltage, mv	70.3	69.7

about 90 $\mu\Omega$/1000 hours. Differences do appear in the behavior of the element resistances and Seebeck voltages between the two lots of material. The main difference is in the slight decrease in bonded element resistance for P33A elements.

C. 1100-Hour Test of Bonded 3N, 3P, and Unbonded 2P Elements

A large group of varied bonded and control elements was put on test at 525°C on June 19, 1968. The initial (for 6/19/68) resistances are listed in Table VI. Some of these elements have been previously tested for varying periods. Also, some of the 3P bonded elements were encapsulated with argon -5% hydrogen to test the effect of the reducing atmosphere on isothermal lifetime behavior.

The entire group of elements was tested for 1100 hours, then taken off test. Only about half the elements were measured at this point. The results of the measurements on these elements are reported here. The initial and 1100 hours resistance values for these elements are listed in Table VII. Table VIII shows the average values of contact and element resistances for the three sets of measured elements.

1. Bonded 3P Elements

Three of the five bonded 3P elements measured were encapsulated in argon - 5% hydrogen. Their performances appear to have been quite acceptable. Excluding the one 400 $\mu\Omega$ contact, which for ordinary purposes is considered to have failed, the other three show decreasing resistance. The over-all performance of the 3P contacts is quite reasonable at an average rate of increase of 18 $\mu\Omega$/1000 hours. The average change in 3P element resistance, 0.12 m Ω, is somewhat less than what has been found in most previous testing.

2. Unbonded 2P

The unbonded 2P elements, encapsulated in argon,

TABLE VI

Resistances of Elements for Isothermal Testing

Element	Top CR $\mu\Omega$	Bottom CR $\mu\Omega$	Element mΩ	
6A4P24	150	200	1.60	*
6A2P24	150	200	1.80	
6A1P24	170	---	1.48	*
6A6P24	150	---	1.45	
6L2P30	---	160	2.04	
616P15	---	450	1.85	*
6L4P30	---	120	1.97	‡
6L5P30	---	400	1.70	*
617P15	240	280	1.96	
5D7P19	375	---	1.88	*‡
5D4P19	340	---	1.71	‡
5C3P19	---	180	1.80	‡
715P37	170	---	1.78	‡
1P25	---	---	2.20	‡
2P25	---	---	2.20	‡
4P33A	---	---	2.45	‡
3P33A	---	---	2.60	‡
5P33A	---	---	2.20	‡
31P37	---	---	2.30	‡
34P37	---	---	2.40	‡

35P37	---	---	2.35 ‡
5P' 16	---	---	0.95
4P' 16	---	---	0.90
11' "16	---	---	0.85
19P' 16	---	---	0.88
5R13N22	85	60	0.735
5R12N22	70	60	0.630
5R7N22	100	70	0.590
5R3N22	---	120	0.530
5R14N22	75	120	0.605
5R8N22	---	95	0.61
5R6N22	---	200	0.62
5R10N22	---	95	0.565
5R9N22	100	120	0.630

* H_2-Ar gas mixture

‡ Previously tested isothermally

Note: P' is the designation for 2P material.

TABLE VII

Average Resistances for 1100 Hour Tested 3P, 2P and 3N Elements

Bonded 3P Elements	0 Hours	1100 Hours
Contact resistance, $\mu\Omega$	205	225
Element resistance, m Ω	1.65	1.77
(H_2-Ar) Contact resistance, $\mu\Omega$	231	235
Unbonded 2P Elements		
Element resistance, m Ω	0.895	0.830
Bonded 3N Elements		
Contact resistance, $\mu\Omega$	84	99
Element resistance, m Ω	0.613	0.5868

TABLE VIII

Resistance Values of Isothermally Tested Elements
Initial and 1100 hours

Element	0 hours			1100 hours		
	CR_T $\mu\Omega$	CR_B $\mu\Omega$	Element mΩ	CR_T $\mu\Omega$	CR_B $\mu\Omega$	Element m Ω
6A1P24*	170	---	1.48	125	---	1.82
6A4P24*	150	200	1.60	145	200	1.655
6A6P24	150	---	1.45	160	---	1.79
6L2P30	---	160	2.04	---	250	1.80
6L5PP30*	---	400	1.70	---	470	1.78
4P' 16	---	---	0.90	---	---	0.66
5P' 16	---	---	0.95	---	---	1.00
11P' 16	---	---	0.85	---	---	0.95
14P' 16	---	---	0.88	---	---	0.71
5R3N22	---	120	.530	---	---	0.500
5R6N22	---	200	.62	---	900	.500
5R7N22	100	70	.590	200	---	.600
5R8N22	---	95	.61	---	150	.530
5R9N22	100	120	.630	30	50	.670
5R10N22	---	95	.565	---	700	.500
5R12N22	70	60	.630	85	30	.555
5R14N22	75	120	.605	200	450	.510
5R13N22	85	60	.735	95	55	.750

* H_2-Ar atmosphere

showed a 7% decrease in room temperature resistance. Since these are the first 2P elements to be tested isothermally, no comparisons can be made.

3. Bonded 3N

The n-type elements tested here represent the first tests at 525°C; previous testing has been mainly at 600°C. The behavior of the n-type contacts is fairly reasonable, considering the results of previous testing. The rate of increase in contact resistance is approximately 14 $\mu\Omega$/ 1000 hours. Junctions tested at 600°C for 4700 hours increased at an average rate of approximately 13 $\mu\Omega$/ 1000 hours. The latter contacts were lower in initial resistance, however, 55 $\mu\Omega$ compared with 84 $\mu\Omega$ for those tested most recently at 525°C.

The element resistance of the n-elements tested at 525°C decreased about 7% in 1000 hours. The elements tested at 600°C decreased (in the case of bonded elements) nearly 8% in 4700 hours.

IV. GRADIENT TESTING OF PbTe COUPLES

A test of fourteen bonded and two unbonded couples was started on February 1, 1968. The test was halted on April 4 due to an anticipated general power shutdown in the laboratory. At this time a number of couples were exchanged, and the atmosphere was changed from pure argon to a 5% H_2-argon mixture on resumption of the test. The test continues at this writing.

A. Couple Life Test II

The original loading for this test consisted of fourteen bonded and two unbonded couples. This test included an internal desiccator filled with P_2O_5 in the bell jar. The initial total resistances of these couples and their resistances after 1400 hours of testing are listed in Table IX. Only two of the fourteen original couples survived with both bonds intact. The others generally had a very weak or nonexistent P-type junction. This was true in the case of couples with fairly low operating resistances, as can be seen in five instances. The deterioration of these junctions is reflected in the averaged performance of twelve of the couples shown in Fig. 22. (This excludes 7G5 and 7F3, since their resistances were extremely high at the end of the test.) The major factor producing the monotonic decrease in power is the increasing internal resistance of the couples, combined with a slight decrease in open circuit voltage.

B. Couple LifeTest III

The next test, which is in part a continuation of couple test II, consisted of seven unbonded couples that had run in the previous test for 1400 hours, two bonded couples from the previous test, four bonded couples with no testing history, and three unbonded 2P-3N couples. All the test couples had tungsten hot straps. A phosphorous pentoxide desiccator was also used in the bell jar for this test. The atmosphere, however, was changed from argon to

TABLE IX

Initial and Final Room Temperature and Operating Resistances of Gradient Tested PbTe Couples - Test II

	0 hours		1400 hours (1)	
Couples	R. T. Resistance mΩ	525° Resistance mΩ	R. T. Resistance mΩ	525° Resistance mΩ
7F8	3.25	12.15		88.5
7G6	3.55	8.8		37.9
7F7	3.55	10.2		23.7
7E1	3.10	9.0		12.7
7G4	3.42	12.1	3.40	8.5
7F6	3.45	7.3		12.1
765	3.30	11.6		____
7F3	3.50	11.8		420
7G2	3.39	9.9		12.2
7G3	3.38	10.9		14.0
7E4	3.42	11.5		21.8
7F1	3.58	9.0	3.60	11.1
7G8	3.44	10.3		29.6
7G1	3.40	9.3		10.5
7E2 *		35.6		470
7F2 *		17.4		____

* Unbonded

(1) Measured after 1400 hours.

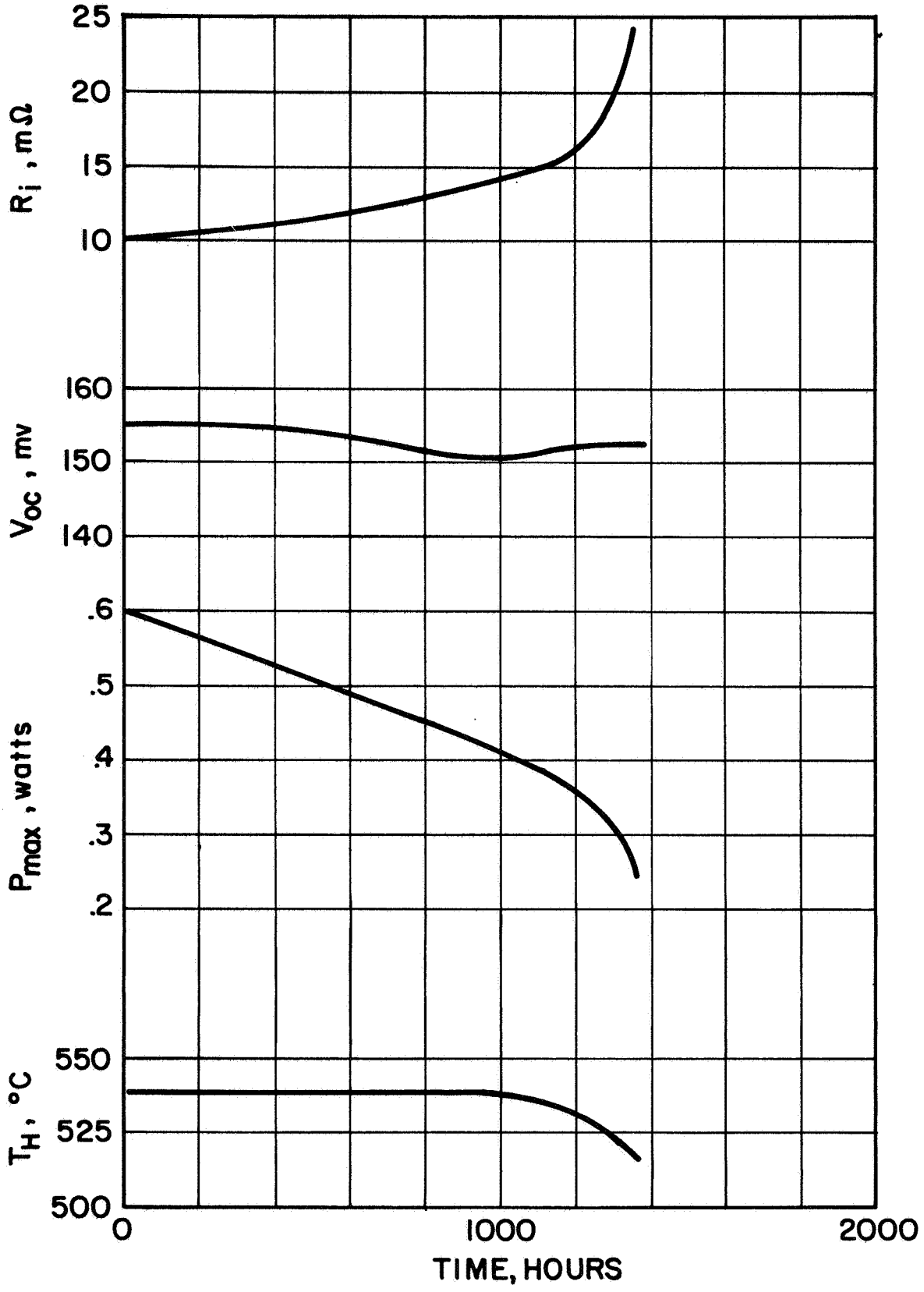

Fig. 22 Average behavior of twelve bonded PbTe (3N-3P) couples during 1400 hour life test in pure argon atmosphere.

a mixture of 95% argon - 5% hydrogen. It was felt that provision of a slightly reducing atmosphere might have a beneficial effect on the performance of the PbTe couples. Shortly after reaching temperature, the leads to the heater of one station shorted together. This eliminated the four stations on that circuit. Thus results are reported on only twelve couples for this test.

The initial room temperature and operating resistances and 1500 hour resistances of these couples are listed in Table X. The room temperature resistance of the unbonded couples is simply the sum of the leg resistances. The room temperature total resistance of an unbonded couple (including contact resistance) is typically 20 - 30 mΩ. The average initial operating resistance for the unbonded couples was 28.5 mΩ, indicating that there is an immediate initial improvement in the contact resistance, since there is about an 8 mΩ increase in resistance of the legs alone at operating temperature. There is also an additional improvement with time. At 1500 hours the average operating resistance was 22.1 mΩ; (this and the initial value excluded 7G1 which was too high to measure at 1500 hours).

The average initial operating resistance of the bonded couples was 13.9 mΩ, a value somewhat higher than is expected. Two couples were apparently defective initially, since values of 17.8 and 25.5 mΩ are what might be expected of pressure-contacted couples. These contributed substantially to the increased initial and 1500 hour average values. However, their increase in resistance with time was quite moderate when compared with previous tests. In the prior test ten bonded couples had an average operating resistance of 9.9 mΩ initially; after 1400 hours, the average resistance of these same ten couples was 26.8 mΩ. Thus, the average rate of increase in internal resistance was 12 mΩ/1000 hours. This is to be compared with an average rate of 0.67 mΩ/1000 hours for those bonded couples tested in the argon-hydrogen atmosphere.

TABLE X

Initial and Operating Resistances for Bonded and Unbonded PbTe Couples Tested in 95% Ar - 5% H_2 Atmoshphere - Test III

Couple	0 hours R. T. Resistance mΩ	0 hours 525° Resistance mΩ	1500 hours 525° Resistance mΩ
765 +	5.85	54.45	43.95
7G6 +	3.80	16.70	10.35
2P-3N #1	1.43	17.35	18.1
7F7 +	3.55	21.70	11.50
7E3 *	3.60	10.30	13.50
7G7 *	4.20	10.25	8.20
7F1 *+	3.60	12.10	11.30
7F4 *	3.50	7.40	9.70
7F5 *	3.50	25.50	28.25
7G4 * +	3.40	17.80	18.55
7G1 +	2.65	11.45	____
7G8 +	2.85	21.20	22.65

* Bonded couples, others unbonded.

\+ Ran during first portion of test for 1400 hours, thus the 1500 hour value here represents 2900 hours for these couples.

Figures 23 and 24 show the average performance of the bonded and unbonded couples of this test. Since a number of these couples had run in the previous test, their performance during the 1400 hours of that test is also shown. In the case of the bonded couples (Fig. 24), this means that the first 1400 hours of data represent only two couples, while the remainder is based on six couples.

The performance of the unbonded couples during the first test, as bonded couples, reflects the general behavior shown in that test (Fig. 22). However, it is clear from Fig. 24 that the addition of hydrogen to the atmosphere has substantially altered the behavior of the pressure-contacted couples. During the first 500 hours of operation in the reducing atmosphere, the average resistance decreased from approximately 25 mΩ to 18 mΩ. Subsequently there has been a very gradual increase in total resistance of about 1 mΩ in 1000 hours. Power output for the unbonded couples during operation under the reducing atmosphere has remained fairly constant at a level approximately half that obtained initially from the couples in a bonded condition. There has been no change in output power during the test with the couples pressure contacted. (There has been a slow decrease in open circuit voltage, which has been somewhat offset by an increase in hot junction temperature.)

The average performance of the bonded couples during the second test (Fig. 24) has been somewhat similar to that of the unbonded couples. There was no initial decrease in resistance, but this is not unexpected. The resistance and open circuit voltage generally follow the trend of the hot junction temperature; however, it is clear from the continued slow decrease in power that the resistance has increased more than the amount due to the rise in ΔT, and that the open circuit voltage has decreased somewhat. The decrease in open circuit voltage can be seen from the curve.

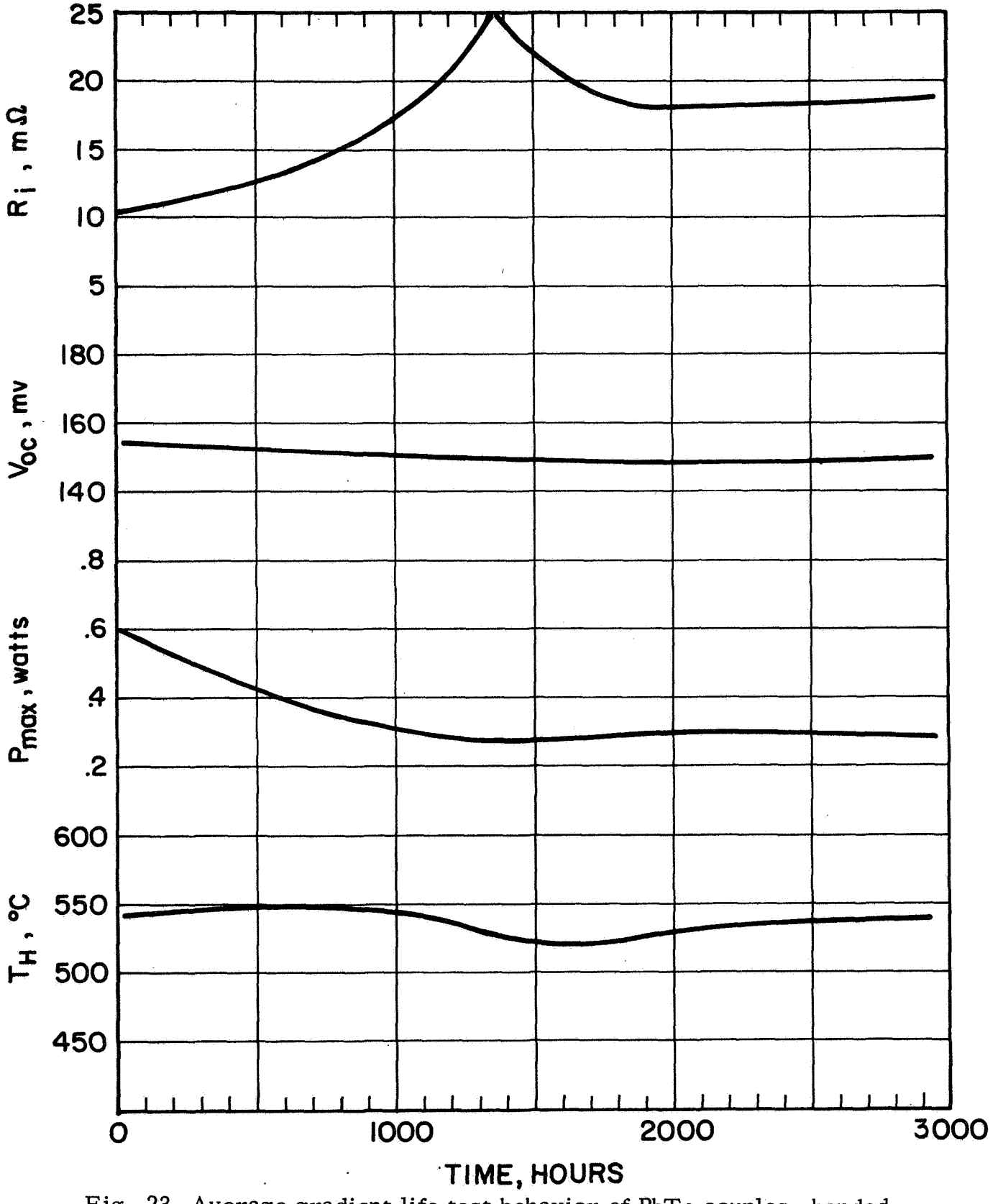

Fig. 23 Average gradient life test behavior of PbTe couples, bonded 0-1400 hours, pressure-contacted 1400-2900 hours under H_2-Ar atmosphere.

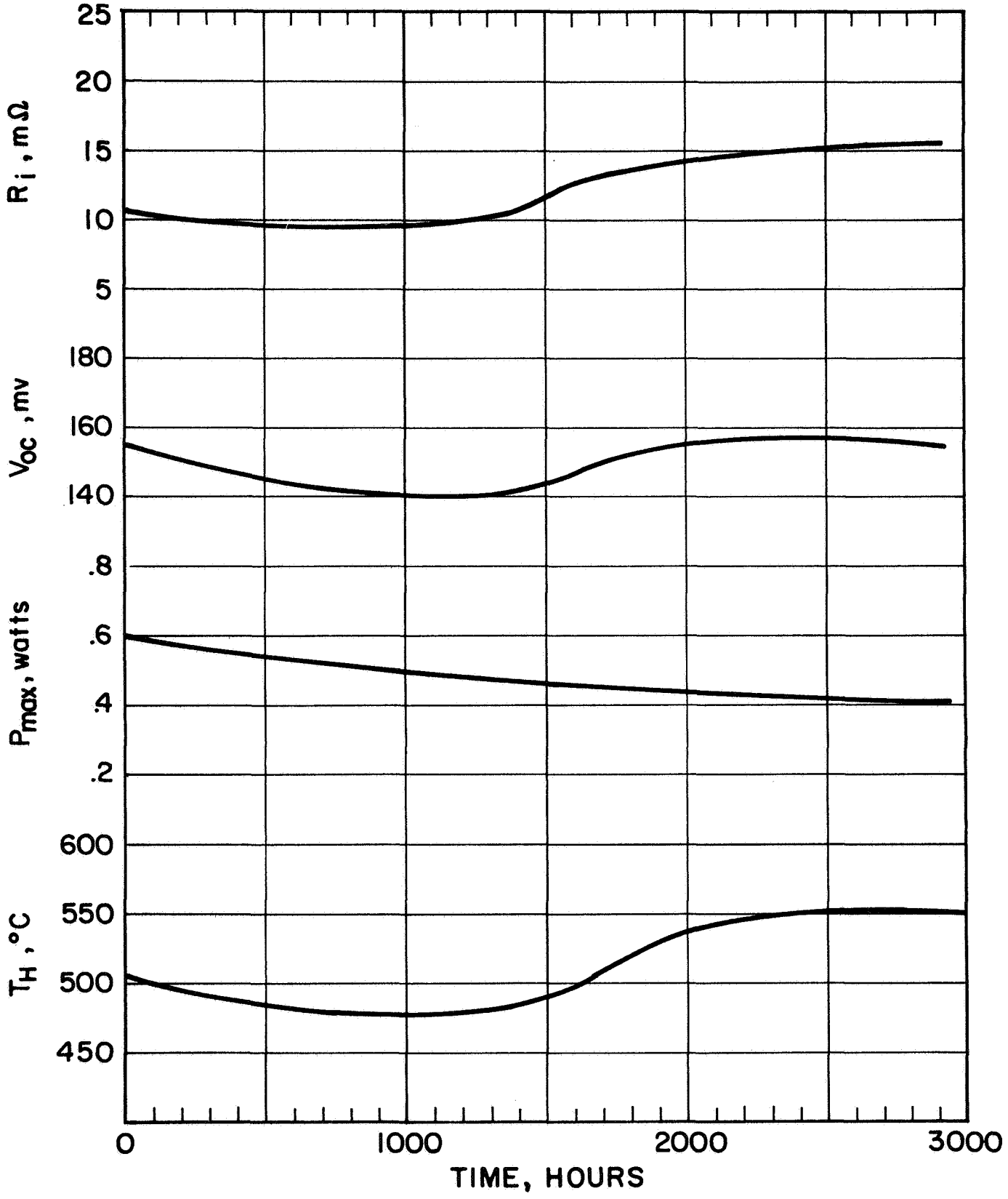

Fig. 24 Average behavior of bonded PbTe couples under H_2-Ar atmosphere 1400-2900 hours. Curve from 0 to 1400 represents two couples of the later six during testing in pure argon.

While the effects of the addition of hydrogen are fairly clear, the mechanism is not. It would appear from the behavior of the unbonded couples, during the period of decreasing internal resistance, that the hydrogen was actively reducing some oxide on the contact surfaces. The latter stage for both types of couple, which seems to be simply a decreased rate of increase in (contact) resistance, is presumably an inhibition of the same process occurring under pure argon. During testing with the argon-hydrogen atmosphere, the P_2O_5 desiccant continued to collect water. Apparently, the hydrogen is able to counteract the effects of water vapor.

Until further testing has been done with the hydrogen-argon mixture, and the thermodynamics of some of the possible reactions which may occur have been examined, no interpretation of these results will be attempted.

V. Si-Ge-PbTe SEGMENTING

Results of measurements on segmented Si-Ge-PbTe couples to a hot junction temperature of 850°C were reported in the First Semiannual Phase Report. These results and previous calculations of various efficiencies were made for a 50°C cold junction temperature for the PbTe. Subsequently, theoretical efficiencies have been calculated for Si-Ge-PbTe and Si-Ge operation between 200°C at the cold side and various hot junction temperatures, up to 1000°C. These results are shown in Fig. 25.

It is clear from the information in Fig. 25 that at the higher cold junction temperature quite substantial benefits are to be derived from segmenting the Si-Ge with PbTe. At a hot junction temperature of 1000°C, the theoretical efficiency for segmented Si-Ge-PbTe is approximately 40% higher than for Si-Ge alone. Segmenting yields only approximately a 10% gain at 1000° when the cold junction is 50°C. Lower hot junction temperatures give larger gains in efficiency from segmenting at the 50°C cold junction temperature. The advantage from segmenting is relatively constant over a range of hot junction temperatures with the 200°C cold junction temperature.

It is quite gratifying to see that substantial benefits may be realized from segmenting when the 200°C cold junction temperature is used, since it is precisely in the radiatively cooled space application that higher efficiency will be of the greatest value.

Design calculations for a segmented couple to operate between 1000°C and 200°C will be presented in a subsequent report.

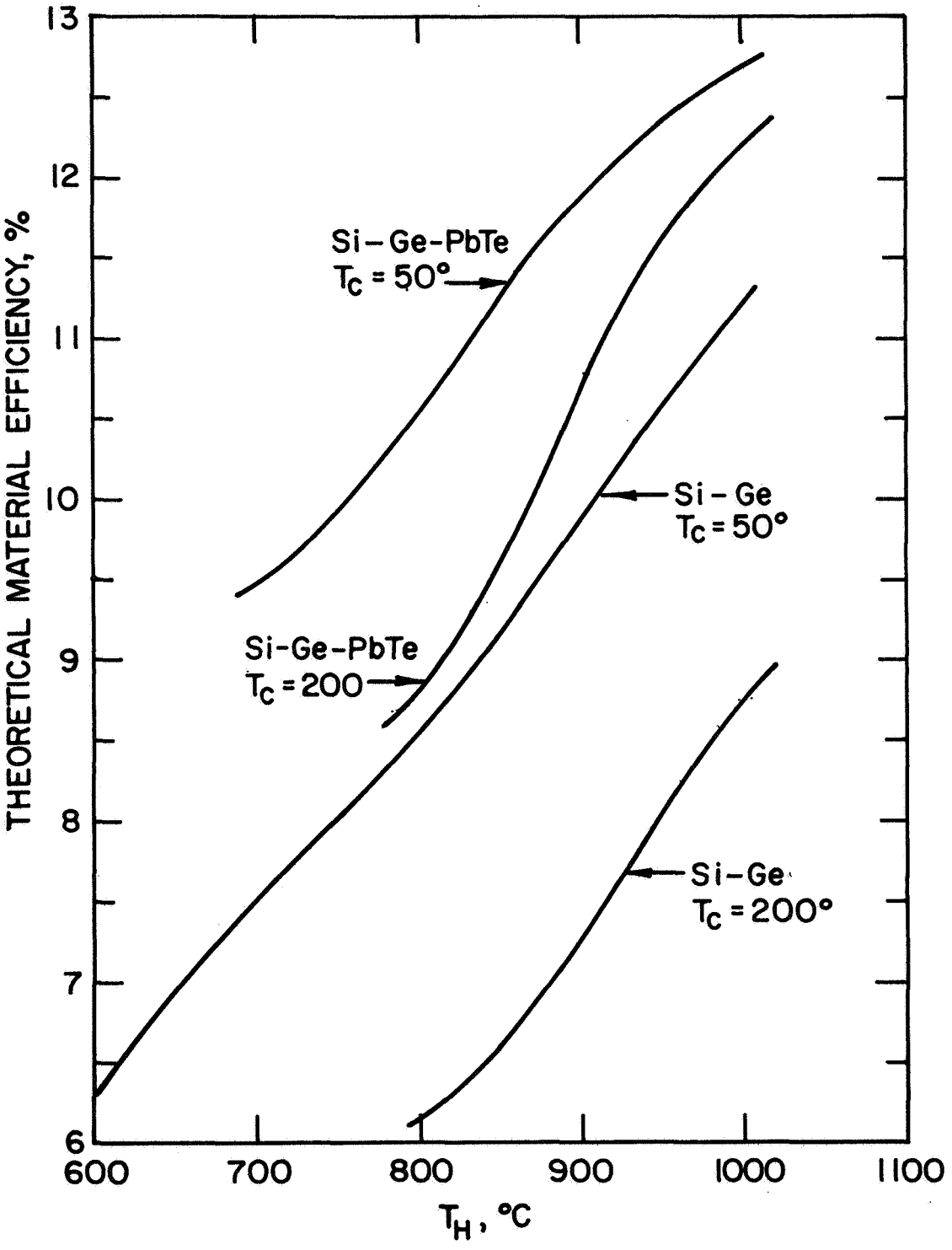

Fig. 25 Theoretical materials efficiency of Si-Ge and segmented Si-Ge-PbTe with 50° and 200° cold junction temperatures.

VI. REFERENCES

1. F. X. Hassion, A. J. Goss and F. A. Trumbore, J. Phys. Chem. 59, 1118 (1955).

2. H. J. Goldschmidt, Interstitial Alloys, Plenum Press, New York 1967 pp. 312-313.

3. W. C. Hagel: Diffusion, in: Intermetallic Compounds, J. H. Westbrook, Editor, John Wiley and Sons, New York 1967 pp. 377 - 404.

4. R. A. Swalin, Thermodynamics of Solids, John Wiley and Sons, New York 1962 pp. 301 - 305.

5. M. Hansen, Constitution of Binary Alloys, MacGraw Hill, New York 1968.

6. R. P. Elliot, Constitution of Binary Alloys, First Supplement, MacGraw Hill, New York 1965.

7. L. H. Brixner, J. Inorg. Nucl. Chem. 24, 257 (1962).

8. M. Chomentowski, H. Rodot, G. Villers and M. Rodot, Compt. Rend. Acad. Sci. Paris, 261, 2198 (1965).

9. J. W. Wagner and J. C. Woolley, Mat. Res. Bull. 2, 1055 (1967).

10. T. C. Harman, Solid State Research, 3, 5 (1967) Lincoln Laboratory MIT, Report under Contract AF19(628)-5167.

11. S. E. R. Hisckocks and P. D. West, Journ. Matls. Science 3, 76 (1968).

12. N. Kh. Abrikosov, K. A. Dvul' dina and T. A. Davilyan Russ. Journal of Inorg. Chemistry 3, 214 (1959).

13. H. A. Johansen, J. Inorg. Nucl. Chem. 6, 344 (1958).

14. D. W. Jonston and D. E. Sestrich, J. Inorg. Nucl. Chem. 19, 229 (1961).

15. A. J. Panson and W. D. Johnson, J. Inorg. Nucl. Chem. 26, 701 (1964).